Neutron Activation Analysis and X-ray Fluorescence of Chert Artifacts from Mielke #1 (33SH26), Shelby County, Ohio

Matthew T. Boulanger

Introduction

Artifacts from the Mielke #1 (33SH26) American Indian archaeological site (Figure 1) in Shelby County, Ohio, were analyzed by X-ray fluorescence (XRF) and by neutron activation (NAA). XRF analyses were performed at the Archaeometry Laboratory at Southern Methodist University, and NAA was conducted at the University of Missouri Research Reactor (MURR). These analyses were performed to explore the suitability of geochemical methods for establishing the provenance (geological source) of the chert artifacts.

Possible Chert Types Present in the Collection

The Mielke #1 artifacts are visually consistent with several different chert sources from across the Midwest. Eren provided a list of potential source identifications based on macroscopic visual classifications. Prior to submitting the specimens for analysis, I also examined each by hand, using a hand lens and reference literature (e.g., Cantin 1994, 2008; Converse 2007; DeRegnaucourt and Georgiady 1998; Stout and Schoenlaub 1946) to identify what appeared to be the most likely source. Results of these visual classifications are reasonably consistent, though they sometimes differ in which specific lithic sources are referenced. For example, Eren suggests that CHR296–305 are visually similar to the Harrodsburg chert of Hardin County, Kentucky. I concur that these samples are similar to Harrodsburg chert, but I believe that they more closely match the Allens Creek chert of southern Indiana (Cantin 2008). Both cherts are Mississippian aged and fossiliferous and may be "indistinguishable even under a microscope" (Cantin 2008:14).

Based on the macroscopic attributes, a number of chert sources in the Midwest are good candidates for comparisons with the Mielke data. These include the Flint Ridge and Plum Run chert, Upper Mercer chert, Zaleski Black flint, Wyandotte and Hopkinsville chert, Holland chert, and Harrodsburg chert. At least two specimens in the Mielke #1 sample are visually consistent with Paoli chert (a.k.a. Carter Cave flint).

Flint Ridge and Plum Run

The Flint Ridge chert source located in southeastern Licking County and western Muskingum County, Ohio, consists of a roughly 8-mile long and 3-mile-wide ridge on which the Vanport Limestone member of the Alleghany Formation (Pennsylvanian) is discontinuously exposed. Lepper et alia (2001:53) describe chert from the Flint Ridge locality as one of the "most widely distributed lithic raw materials in eastern North America" and suggest that American Indians first began quarrying here more than 10,000 years ago during the Paleoindian period. Luedtke (1976:230) lists several of the known prehistoric quarry areas, as do Georgiady and Brockman (2002:99–100), DeRegnaucourt and Georgiady (1998:52*ff*), and Converse (2007:168–173).

Chert from the Vanport Member outcrops along Flint Ridge exhibits a wide variety of macroscopic traits (i.e., color, texture, opacity, luster), and various colloquial "varieties" of this chert are commonly used by geologists and archaeologists. Specimens discussed in this study represent several of these varieties, including the Flint Ridge Flint, Flint Ridge Chalcedony (a.k.a. Flint Ridge White), and Flint Ridge Nethers Farm (a.k.a. Pinstripe). Readers are referred to Carlson (1987, 1991), Converse (2007), DeRegnaucourt and Georgiady (1998), and Lepper et alia (2001) for descriptions of the macroscopic traits associated with each of these names.

Despite deriving from the same limestone as Flint Ridge chert, Plum Run chert is often treated by archaeologists as a distinct raw material because of perceived differences in coloration (Murphy and Blank 1970). Luedtke (1976:235) states that material from Plum Run (her "Locality 4") is thinner, of poorer quality than that which is available at Flint Ridge, and mostly blue-gray in color weathering to brown. Luedtke's (1976) previous use of NAA of Flint Ridge and Plum Run cherts found that the Plum Run specimens were enriched in Lu, Zn, and Cr relative to Flint Ridge, suggesting to her that further geochemical studies of these materials may be warranted.

Upper Mercer Chert

Luedtke (1976, 1992) describes chert form the Upper Mercer Limestone (Pottsville Formation, Pennsylvanian) as occurring in beds up to 15 cm thick within a limestone and shale matrix. Upper Mercer chert is typically black (N/2) to dark gray. Mottles of lighter colors are frequently observed in the chert, as are veins of white–blue chalcedony. Variations in color and amount of mottling have been used to define several varieties of the chert, including "Coshocton Black," "Coshocton Gray," "Nellie," and "Bird-Dropping" (see Converse 2007; DeRegnaucourt and Georgiady 1998). As with Flint Ridge chert, there is only mild consensus on the necessary and sufficient conditions of each variety, and it is unclear whether the "varieties" are discreet geological packages or simply continuous variation within the overall formation.

Wyandotte and Hopkinsville Chert

The lower portion (approx. 80 ft) of the Ste. Genevieve Limestone (Mississippian aged) consists of bedded limestone with abundant fine-grained nodular and ball-shaped chert masses ranging from 1 to 8 inches in diameter. This chert-rich zone is classified as the Fredonia Member of the Ste. Genevieve Limestone (see Bassett and Powell 1984). Chert is particularly abundant in the upper portions of the Fredonia Member. Well-known exposures of this chert-rich limestone occur in Harrison County, Indiana, where the exposed chert is referred to by archaeologists as "Wyandotte chert," for exposures at Wyandotte Cave, and near the town of Hopkinsville, Christian County, Kentucky, where the chert is referred to by archaeologists as "Hopkinsville chert." Synonyms for this chert include "Indiana Hornstone" and "Harrison County chert."

Luedtke (1976) describes chert from the Fredonia Member as typical medium blue-gray (5B 5/1) in color, with a fine texture and shiny luster. She notes that concentric banding is sometimes present within nodules. Tankersley (1985, 1989) suggests that Wyandotte chert is mineralogically distinctive from other look-alike cherts in the Midwest, though he does not include samples from near Hopkinsville in his analysis. Previous uses of NAA to examine chert from the Fredonia Member have been restricted to source specimens from southern Indiana (e.g., Boulanger et al. 2015; Luedtke 1976) but have been promising in the distinction of this material from other midwestern cherts.

Holland Chert

The Pennsylvanian-aged Holland Limestone (Staunton Formation, Raccoon Creek Group) is the source for at least two colloquial varieties of chert discussed in the archaeological literature. So-called Holland chert is a bluish-gray chert that crops out in Dubois County, Indiana. DeRagnaucourt and Georgiady (1998) suggest that this material can vary substantially in color from black to pinkish gray. Darker varieties of this chert are often referred to as Ferdinand chert or Holland Dark Phase (e.g., White 2002). Cantin (1994, 2008) states that this darker variety of chert from the Holland Limestone is macroscopically similar to chert from the Upper Mercer Limestone in Ohio. Given that the Holland and Upper Mercer Limestones are of the same approximate age, stratigraphy, and lithology, this is not particularly surprising.

Harrodsburg and Allens Creek Chert

Highly fossiliferous and oolitic chert from the Harrodsburg Limestone (Mississippian aged) in Hardin County, Kentucky, is known to have been used by American Indian stone-tool makers. According to Cantin (2008), Harrodsburg chert is usually described as being white to light gray in color, though some specimens shade into brown and very dark gray. The highly fossiliferous groundmass of Harrodsburg chert makes it visually distinctive. Fossils such as crinoids and bryzoans are common in the chert, making it difficult to distinguish from so-called Allens Creek chert from the Mississippian-aged Muldraugh Formation, which crops out in Monroe County, Indiana. Like chert from the Harrodsburg Limestone, Allens Creek chert is highly fossiliferous and light gray in color. Cantin (1994, 2008) describes Allens Creek chert as having a fine texture and being well silicified, in contrast to Harrodsburg chert, which is described as being somewhat blocky and poorly cemented.

Burlington Chert

Chert from the Burlington Limestone (Mississippian aged) is usually a white, coarse-grained, and crinoidal chert found in outcrops in the Mississippi River valley and stretching westward across the rim of the Ozarks into Oklahoma and Arkansas. Numerous American Indian quarries into the Burlington chert have been identified in the Midwest, though much attention has been given to the Crescent Hills Quarry (23SL16) in west-suburban St. Louis County (Ives 1975). Comparative NAA data for Burlington chert comes from samples collected by Ives but analyzed in the 1990s as part of a later study. Burlington chert is also easily obtained along riverbeds and creekbeds in western Illinois and eastern Missouri. The chert is most often white to bluish white in its unmodified form, but heat treatment often results in a red-pink hue with a distinctive waxy luster.

X-ray Fluorescence Analysis

All the formal tools and preforms collected from Mielke were subjected to nondestructive analysis using an XRF spectrometer. These artifacts include complete and broken fluted points, gravers, and late-stage bifaces.

Analytical Protocols

Each specimen was analyzed using a Bruker Tracer 5i handheld portable X-ray fluorescence spectrometer. The Tracer 5i uses a Rh-based X-ray tube operating at 50 kV at 35 μa and a silicon drift detector. The X-ray beam was collimated to approximately 8 mm. Spectra collected by the spectrometer are quantified using a custom calibration based on a suite of 43 well-characterized obsidian reference specimens developed by the Archaeometry Laboratory at the University of Missouri (Glascock and Ferguson 2012; Speakman 2012). Artifact specimens are analyzed on the Tracer 5i for at least 90 s. This protocol and the obsidian calibration routine permit quantification of the following minor and trace elements: Ti, Mn, Fe, Zn, Ga, Rb, Sr, Y, Zr, Nb, Ba, and Th. A solid piece of Glass Mountain Rhyolite obsidian was used as a check standard for these analyses. The United States Geological Survey distributes a powdered version of this same material for its RGM-1 and RGM-2 certified reference material, and a comparison of my analysis of it with reference values is provided in Table 1.

After data collection and quantification, element concentration data were tabulated in parts per million using Microsoft® Office Excel. These data are provided in Table 1 and Table 2.

XRF Results and Discussion

The nondestructive XRF analyses suggest that the measured elements are at or below detection limits of the calibration in nearly all the specimens. The only elements consistently above detection limits in all specimens are Fe and Y, and Sr was quantified in 92% of the specimens. None of these elements appears to show appreciable differences relating to the suspected provenance of the chert. Ga and Th were below detection limits (≈1 ppm) in all the specimens, and the remaining elements were below detection limits in 50%–97% of the sample.

The results suggest that, at least when applied to cherts from these suspected sources, nondestructive XRF is likely not a viable method for pursuing provenance-related research. It should be noted that the calibration and technique used here are optimized for obsidian-related provenance studies and focus on mid-Z elements, which tend to be diagnostic of obsidian sources. Yet, these same elements—especially Rb, Sr, Th, and Ba—have proven helpful in defining chert-source groups in other studies. Detection limits for these elements in our current calibration range from 1 ppm (Sr and Th), 5 ppm (Rb), and ≈500 ppm (Ba). Thus, the concern with whole-sample XRF analysis of these cherts is not necessarily the selection of elements but the limitation of the instrumental method itself to detect trace amounts of these elements. Further studies of these particular chert sources may focus on major and minor elements, as these may be easier to quantify by nondestructive XRF; however, these elements are also less useful for distinguishing specific sources.

Neutron Activation Analysis

Included in the sample of artifacts subjected to NAA are a range of debitage classes, expedient tools, and formal tools (Table 3). Previous applications of NAA to chert sources in the Midwest have been reasonably successful at distinguishing distinct compositional groups that represent individual quarries or quarrying areas. Here, I compare data from the Mielke #1 artifacts to the database of sources analyzed by NAA at MURR. When possible, I integrate data from previous studies performed at MURR (e.g., Boulanger 2018, 2019; Boulanger et al. 2015; Chiarulli and Katz 2016; Glascock 2004; Morrow et al. 1992).

Specimen Preparation

Prior to shipment to MURR, specimens were inventoried and assigned laboratory analytical identifiers (ANIDs) CHR296–357, sequential. The archaeological artifacts were sampled at MURR by removing a small portion with a diamond-edged rock saw. Cut sections were further reduced in size by placing them between two tool-steel plates and crushing them in a Carver Press. Several small 50–100 mg fragments were obtained from the crushed specimens. Fragments were examined under low-power magnification, and fragments with metallic streaks or crush fractures were eliminated from consideration. Several grams of the remaining fragments were obtained from each sample and temporarily stored in plastic bags. Several of the specimens were simply too small to sample without sacrificing the entire artifact; however, a majority of pieces were of sufficient size to permit preservation of the remaining artifact.

Two analytical samples were prepared from each specimen. Portions of approximately 100 mg of rock fragments were weighed into high-density polyethylene vials used for short irradiations at MURR. At the same time, 700 mg aliquots from each specimen were weighed into high-purity quartz vials used for long irradiations. Individual sample weights were recorded to the nearest 0.01 mg using an analytical balance. Both vials were sealed prior to irradiation. Along with the unknown samples, standards made from National Institute of Standards and Technology (NIST) certified standard reference materials of SRM-1633b (Coal Fly Ash), SRM-278 (Obsidian Rock), and SRM-688 (Basalt Rock) were similarly prepared.

Irradiation and Gamma-Ray Spectroscopy

Neutron activation analysis of most archaeological samples at MURR, which consists of two irradiations and a total of three gamma counts, constitutes a superset of the procedures used at most other NAA laboratories (Glascock 1992; Glascock and Neff 2003; Neff 2000).

As discussed in detail by Glascock (1992), a short irradiation is carried out through the pneumatic tube irradiation system. Samples in the polyvials are sequentially irradiated, two at a time, for 5 seconds by a neutron flux of 8×10^{13} n cm^{-2} s^{-1}. The 720-second count yields gamma spectra containing peaks for nine short-lived elements: aluminum (Al), barium (Ba), calcium (Ca), dysprosium (Dy), potassium (K), manganese (Mn), sodium (Na), titanium (Ti), and vanadium (V).

The long-irradiation samples are encapsulated in quartz vials and are subjected to a 70–hour irradiation at a neutron flux of 5×10^{13} n cm^{-2} s^{-1}. This long irradiation is analogous to the single irradiation utilized at most other laboratories. After the long irradiation, samples decay for 7 days and then are counted for 1,800 seconds (the "middle count") on a high-resolution germanium detector coupled to an automatic sample changer. The middle count yields determinations of seven medium half-life elements—namely, arsenic (As), lanthanum (La), lutetium (Lu), neodymium (Nd), samarium (Sm), uranium (U), and ytterbium (Yb). After an additional 3- or 4-week decay, a final count of 8,500 seconds is carried out on each sample. The latter measurement yields the following 17 long half-life elements: cerium (Ce), cobalt (Co), chromium (Cr), cesium (Cs), europium (Eu), iron (Fe), hafnium (Hf), nickel (Ni), rubidium (Rb), antimony (Sb), scandium (Sc), strontium (Sr), tantalum (Ta), terbium (Tb), thorium (Th), zinc (Zn), and zirconium (Zr).

The element concentration data from the three measurements were tabulated in parts per million (ppm) using Microsoft® Office Excel. Contextual and descriptive data for the specimens are appended to the concentration spreadsheet to facilitate organizing, sorting, and extracting sample information. Additional copies of these data are available upon request to the Archaeometry Laboratory, following the Archaeometry Laboratory's *Data Management and Sharing Plan* (Boulanger and Stoner 2012).

Interpreting Chemical Data

Analyses at MURR described previously typically produce elemental concentration values for 33 elements. However, it is often the case that some elements are at or below detection limits in cryptocrystalline silicates, such as chert and jasper, which are upwards of 99% SiO2. The chemical data generated here show a high number of elements that are at or below detection limits (nondetects) for MURR techniques and instrumentation. Nondetected values were replaced using a data-augmentation algorithm based on a truncated additive logistic normal distribution within a Bayesian framework. In short, Markov chain Monte Carlo (MCMC) simulation is used to sample the joint posterior distribution of nondetected elements, using the estimated detection limits as a prior (Palarea-Albaladejo and Martín-Fernández 2015; Palarea-Albaladejo et al. 2014). Estimated detection limits for chert specimens previously analyzed at MURR are not preserved. With these so-called legacy data, replacement values for nondetected elements were calculated using a Mahalanobis-distance-minimizing model described by Neff (2002).

Some legacy data sets are missing abundances for elements not because of detection limits but because these elements were not quantified during analysis. Data for the Wyandotte and Flint Ridge chert sources reported by Morrow et alia (1992) and Glascock (2004) do not have values for the following elements: Ti, Ni, and Zr. These elements were removed from all the data sets to allow direct comparability. We note, however, that Wyandotte chert samples previously analyzed by NAA at MURR exhibit concentrations of Ti and Zr that help distinguish this material from other chert sources in the Midwest. Similarly, specimens of Flint Ridge White and Holland chert have abundances of K and V that are at or below the limits of detection. These elements were also removed from the data set before statistical analysis.

Calculations and statistical analyses were performed on base-10 logarithms of the elemental abundance data. Use of log concentrations rather than raw data compensates for differences in magnitude between the major elements (e.g., Al, Na, and Fe) and trace elements (e.g., rare earth elements [REEs]). Transformation to base-10 logarithms also yields a more normal distribution for many trace elements (Luedtke 1992; see also Limpert et al. 2001).

The interpretation of compositional data obtained from the analysis of archaeological materials is discussed in detail elsewhere (e.g., Baxter and Buck 2000; Bieber et al. 1976; Bishop and Neff 1989; Glascock 1992; Harbottle 1976; Neff 2000) and will only be summarized here. The main goal of data analysis is to identify distinct homogeneous groups within the analytical database. Based on the provenance postulate of Weigand et alia (1977), different chemical groups may be assumed to represent geographically restricted sources. For lithic materials such as obsidian, basalt, and cryptocrystalline silicates (e.g., chert, flint, or jasper), raw material samples are frequently collected from known outcrops or secondary deposits and the compositional data obtained is used to define the source localities or boundaries. The locations of sources can also be inferred by indirect methods such as the "criterion of abundance" (Bishop et al. 1982) or by arguments based on geological and sedimentological characteristics. The ubiquity of ceramic raw materials usually makes it impossible to sample all potential "sources" intensively enough to create groups of knowns to which unknowns can be compared. Moreover, there is no guarantee that the exact geological locality from which clay and/or temper was prehistorically obtained is available today. Changes in land use (e.g., deforestation, cultivation, and urbanization) and in landscapes (e.g., damming of major rivers, terraforming to construct highways) may obscure, destroy, or otherwise make inaccessible prehistorically used clay resources. Thus, many projects involving analyses of ceramic artifacts rely on inference to construct groups of specimens with similar elemental compositions.

Compositional groups can be viewed as "centers of mass" in the compositional hyperspace described by the measured elemental data. Groups are characterized by the locations of their centroids and the unique relationships (i.e., correlations) between the elements. Decisions about whether to assign a specimen to a particular compositional group are based on the overall probability that the measured concentrations for the specimen could have been obtained from that group.

Initial hypotheses about source-related subgroups in the compositional data can be derived from noncompositional information (e.g., archaeological context, decorative attributes, etc.) or from application of various pattern-recognition techniques to the multivariate chemical data. Some of the pattern-recognition techniques that have been used to investigate archaeological data sets are cluster analysis (CA), principal components analysis (PCA), and discriminant analysis (DA). Each of the techniques has its own advantages and disadvantages that may depend on the types and quantity of data available for interpretation.

The variables (measured elements) in archaeological and geological data sets are often correlated and frequently large in number. This makes handling and interpreting patterns within the data difficult. Therefore, it is often useful to transform the original variables into a smaller set of uncorrelated variables in order to make data interpretation easier. Of the above-mentioned pattern-recognition techniques, PCA is the technique that transforms the data from the original correlated variables into uncorrelated variables most easily.

Principal components analysis creates a new set of reference axes arranged in decreasing order of variance subsumed. The individual PCs are linear combinations of the original variables. The data can be displayed on combinations of the new axes, just as they can be displayed on the original elemental concentration axes. PCA can be used in a pure pattern-recognition mode (i.e., to search for subgroups in an undifferentiated data set) or in a more evaluative mode (i.e., to assess the coherence of hypothetical groups suggested by other criteria). Generally, compositional differences between specimens can be expected to be larger for specimens in different groups than for specimens in the same group, and this implies that groups should be detectable as distinct areas of high point density on plots of the first few components.

Principal components analysis of chemical data is scale dependent, and analyses tend to be dominated by those elements or isotopes for which the concentrations are relatively large. As a result, standardization methods are common to most statistical packages. A common approach is to transform the data into logarithms (e.g., base 10). As an initial step in the PCA of most chemical data at MURR, the data are transformed into log concentrations to equalize the differences in variance between the major elements, such as Al, Ca, and Fe, on one hand and trace elements, such as the rare-earth elements (REEs), on the other hand. An additional advantage of the transformation is that it appears to produce more nearly normal distributions for the trace elements.

One frequently exploited strength of PCA, discussed by Baxter (1992), Baxter and Buck (2000), and Neff (1994; 2002), is that it can be applied as a simultaneous R- and Q-mode technique, with both variables (elements) and objects (individual analyzed samples) displayed on the same set of principal component reference axes. A plot using the first two principal components as axes is usually the best possible two-dimensional representation of the correlation or variance-covariance structure within the data set. Small angles between the vectors from the origin to variable coordinates indicate strong positive correlation; angles at 90° indicate no correlation; and angles close to 180° indicate strong negative correlation. Likewise, a plot of sample coordinates on these same axes will be the best two-dimensional representation of Euclidean relations among the samples in log-concentration space (if the PCA was based on the variance-covariance matrix) or standardized log-concentration space (if the PCA was based on the correlation matrix). Displaying both objects and variables on the same plot makes it possible to observe the contributions of specific elements to group separation and to the distinctive shapes of the various groups. Such a plot is commonly referred to as a "biplot" in reference to the simultaneous plotting of objects and variables. The variable interrelationships inferred from a biplot can be verified directly by inspecting bivariate elemental concentration plots.

Whether a group can be discriminated easily from other groups can be evaluated visually in two dimensions or statistically in multiple dimensions. A metric known as the Mahalanobis distance (or generalized distance) makes it possible to describe the separation between groups or between individual samples and groups on multiple dimensions. The Mahalanobis distance of a specimen from a group centroid (Bieber et al. 1976; Bishop and Neff 1989) is defined by

$$D_{y,X}^2 = (y - \bar{X})^t I_x (y - \bar{X}),$$

where y is the 1 × m array of logged elemental concentrations for the specimen of interest, X is the n × m data matrix of logged concentrations for the group to which the point is being compared with $\bar{X}$ being its 1 × m centroid, and I_x is the inverse of the m × m variance-covariance matrix of group X. Because Mahalanobis distance takes into account variances and covariances in the multivariate group, it is analogous to expressing distance from a univariate mean in standard deviation units. Like standard deviation units, Mahalanobis distances can be converted into probabilities of group membership for individual specimens. For relatively small sample sizes, it is appropriate to base probabilities on Hotelling's T^2, which is the multivariate extension of the univariate Student's *t*.

When group sizes are small, Mahalanobis distance-based probabilities can fluctuate dramatically depending on whether or not each specimen is assumed to be a member of the group to which it is being compared. Harbottle (1976) calls this phenomenon "stretchability" in reference to the tendency of an included specimen to stretch the group in the direction of its own location in elemental concentration space. This problem can be circumvented by cross-validation, that is, by removing each specimen from its presumed group before calculating its own probability of membership (Baxter 1994; Leese and Main 1994). This is a conservative approach to group evaluation that may sometimes exclude true group members.

Small sample and group sizes place further constraints on the use of Mahalanobis distance: with more elements than samples, the group variance-covariance matrix is singular thus rendering calculation of I_X (and D^2 itself) impossible. Therefore, the dimensionality of the groups must somehow be reduced. One approach would be to eliminate elements considered irrelevant or redundant. The problem with this approach is that the investigator's preconceptions about which elements should be discriminate may not be valid. It also squanders the main advantage of multielement analysis—namely, the capability to measure a large number of elements. An alternative approach is to calculate Mahalanobis distances with the scores on principal components extracted from the variance-covariance or correlation matrix for the complete data set. This approach entails only the assumption, entirely reasonable in light of the above discussion of PCA, that most group-separating differences should be visible on the first several PCs. Unless a data set is extremely complex, containing numerous distinct groups, using enough components to subsume at least 90% of the total variance in the data can be generally assumed to yield Mahalanobis distances that approximate Mahalanobis distances in full elemental concentration space.

NAA Results and Discussion

Chert and other cryptocrystalline silicates are often difficult to examine using geochemistry. This is because the abundances of most elements (except Si) are exceedingly low, and specific geological outcrops show highly variable chemistries that overlap with those of other outcrops in multivariate space. The sources discussed herein are no different, and these issues are compounded by two additional problems.

First, the numbers of specimens representing each source sample are variable: Harrodsburg chert is represented by just three specimens, whereas the sample of Wyandotte chert comprises 44 specimens. This variation in sample size makes it difficult to directly compare individual sources, and it prevents direct comparison of artifacts to all sources using elemental abundances and multivariate statistics (e.g., the Mahalanobis distance).

Second, samples assigned to a specific source can show extreme heterogeneity, and there is currently insufficient information about the origins of some specimens in the MURR database to make informed decisions about how to treat this variation. Figure 2 illustrates this second issue well. For the most part, individual chert sources shown in the figure can be distinguished from each other based on their concentrations of Rb and Cs—two highly correlated elements. However, the Flint Ridge compositional group encompasses the compositional space of all other chert sources. Of course, Flint Ridge chert is highly variable in terms of color, texture, and mineralogy. Some variability is to be expected. However, many of the specimens that are relatively higher in Rb and Cs (>4 ppm and >0.1 ppm, respectively) derive from the Plum Run quarries in Mahoning County, suggesting that some of the chemical variation seen here may be attributable to spatial variation in the Vanport Limestone—an interesting observation as it may allow us to distinguish chert of the Plum Run quarries from chert of the Flint Ridge quarries. However, other specimens showing similarly high Rb and Cs concentrations are identified simply as “Flint Ridge chert” and are not attributed to a specific quarry, meaning they could be from Flint Ridge, Plum Run, or some other locality.

As shown in Figure 3, all the concerns expressed above manifest in the current attempt to assign artifacts from Mielke #1 to a particular chert source. Nearly all the Mielke #1 artifacts fall within the confidence ellipse for the Flint Ridge source—but so do all the other sources. Thus, we cannot make source assignments for the artifacts blindly using only the geochemical data. Instead, I recommend an approach that relies on multiple lines of evidence. As discussed above, this approach includes statistical analyses of the raw geochemical data, multivariate transformations and statistical analyses, and visual megascopic characteristics of the chert artifacts.

Principal components analysis of the elemental abundance data for the Mielke #1 artifacts and the chert-source specimens indicates that eight components explain more than 90% of the cumulative variation in the data (Table 4). The first component explains 56.42% of the variance and is strongly loaded on Al, As, Dy, Na, and U. Significant loading on U is attributable to samples of Wyandotte and Hopkinsville chert, which are significantly enriched in this element. Principal component #2 accounts for 13.01% of the variance in the data set. This component is negatively loaded on several transition metals (Co, Fe, Mn, Zn) and positively loaded on REEs, Sb, and U. The relationship between these components, their loading elements, and the chert specimens is shown in Figure 4. Of note in this figure is that nearly all the Mielke #1 artifacts fall within the compositional space defined by the sources used here, indicating that none of the artifacts are clearly geochemical outliers that may be attributed to a source not represented in our data. This is consistent with visual examination of the artifacts, though it does not necessarily rule out the possibility that some of the artifacts derive from look-alike chert sources whose chemistry is similar to the sources discussed here.[1]

Ten artifacts from Mielke #1 (CHR296–305) are visually similar to the Harrodsburg chert of Hardin County, Kentucky. Though, as discussed above, this material is visually similar to Allens Creek chert in Indiana. The ten artifacts analyzed here can be distinguished from the

[1] This is an obvious shortcoming of *all* geochemical studies: “Sourcing” artifacts is entirely dependent on the scope and extent of the sources to which artifacts are compared.

three specimens of Harrodsburg chert currently in the MURR database based on lower concentrations of Al, Fe, and Mn. Nine of the artifact specimens appear to form a distinct group, indicating that they all share more or less the same chemical composition (Figure 5). Specimen CHR 297 (sample no. 2) is chemically distinct from the remaining nine artifacts. These results can be interpreted in a number of ways: (1) The current source sample of Harrodsburg chert does not capture the full range of elemental variability present in this material, and the artifacts are Harrodsburg chert but outside the range of this material as represented by our three source specimens or (2) the current source sample of Harrodsburg chert *does* capture the full range of elemental variability present in this material, and the artifacts are outside this range and are thus not Harrodsburg chert (and perhaps Allens Creek chert). Without additional source specimens of both the Harrodsburg and Allens Creek materials, we likely will not be able to resolve between these two possibilities. However, for the moment, it is possible to state that the Mielke #1 artifacts (CHR296–305) are visually consistent with Harrodsburg/Allens Creek chert and that nine of these artifacts form a distinct cluster of samples that is broadly similar to, but geochemically distinct from, the Harrodsburg source samples from Kentucky. Given the visual and geochemical similarities of these nine samples, it seems reasonable to conclude that they all derive from similar geological provenance.

Nine of the artifacts from Mielke #1 were visually classified as Upper Mercer chert by Eren. Based on visual characteristics such as color, luster, and the presence of microfossils, I classify these same pieces as belonging to several variants (as discussed by Converse 2007) of Upper Mercer chert, including "Bird-Dropping" (CHR306), Coshocton Gray (CHR307), Upper Mercer Blue (CHR308), and Coshocton Black (CHR311–313). However, I would have classified CHR309, -310, and -314 as being either Wyandotte or Holland (dark phase) chert. The chemical compositions of these nine pieces suggest that a majority (n = 8) are consistent with the sample of Upper Mercer chert in the MURR database (Figure 6). Only CHR310 consistently plots within the 90% confidence ellipse for the sample of Wyandotte chert, and it exhibits the same high-uranium profile that appears to distinguish Wyandotte chert from other midwestern cherts. In some projections of these data, specimen CHR309 falls close to the sample of Holland chert currently in the MURR database.

Eight specimens (CHR315–322) were classified visually by Eren as being of Flint Ridge chert. My own classification of these, based on visual characteristics, is the same excepting CHR315, which I believe to be visually consistent with heat-treated Burlington chert. Based on their chemistry alone, it is difficult to confidently associate these eight pieces with either Flint Ridge or Burlington. Although the main Flint Ridge sample and the Burlington sample are chemically distinct, the white and translucent variety of Flint Ridge (so-called Flint Ridge White) is not chemically distinct from Burlington chert in bivariate and PCA space. Plotting the Mielke #1 artifacts against these source groups in bivariate and multivariate space (Figure 7) reveals that they are all consistent with the main Flint Ridge compositional group; however, as noted above, this group is so heterogenous that it subsumes nearly the entirety of compositional space for all sampled midwestern cherts. Based on the chemistry of the pieces as well as their visual similarities to Flint Ridge materials, it seems likely that these eight artifacts can, at least provisionally, be considered to be made on Flint Ridge chert, both the main variety and the specific white variety. Though my own informed opinion is that CHR315 exhibits the opaqueness, waxy luster, coloration (pearlish white to pinkish red), and iron staining consistent with Burlington chert, the geochemical data available provide for only an equivocal match.

Eren classified 18 of the Mielke #1 artifacts (CHR323–340) as being visually consistent with Wyandotte chert from Indiana. Based on visual criteria alone, I agree that CHR323–329 and CHR331 are consistent with Wyandotte chert. Some of these pieces, I believe, are more consistent with Holland chert based primarily on the degree of mottling and the coloration (CHR330, -333, -334, -336, -338, and -339). Specimen CHR332 is, I believe, better described as consistent with the Nethers Farm or Pinstripe variety of Flint Ridge chert. Based on visual characteristics alone, I do not feel confident assigning the remaining pieces (CHR335, -337, and -340) to either the Wyandotte source or the Holland source. In my opinion, they could be from either.

In bivariate (Figure 8 and Figure 9) and multivariate space (Figure 10), the geochemical data suggest that the 18 artifacts visually classified as Wyandotte split into at least two distinct groups. One of these groups consistently plots within the 90% confidence ellipse of the Wyandotte source sample, though because the Hopkinsville chert sample is subsumed entirely by the Wyandotte sample, these two sources cannot yet be discriminated. The second group of artifacts is more difficult to associate with a single chert source group. This is largely because the Upper Mercer (Coshocton Co.) source sample and the Flint Ridge sample overlap significantly in most dimensions. Given that Upper Mercer and Flint Ridge cherts are generally considered to be visually distinctive (e.g., Converse 2007) and that to the best available knowledge only Upper Mercer appears to overlap with Wyandotte in terms of coloration and luster, it seems reasonable to conclude that this second group of artifacts is most likely Upper Mercer chert. The single exception to this may be CHR332, which, as noted above, exhibits the characteristic “pinstripe” coloration common to the Nethers Farm variety of Flint Ridge chert. I am unaware of similar coloration in either Upper Mercer or Wyandotte chert. This artifact consistently plots within the 90% confidence ellipse of the Flint Ridge compositional group. Thus, visual characteristics as well as geochemistry suggest this is an appropriate assignment for the artifact.

Fifteen of the Mielke #1 artifacts are made on a gray-to-white chert with iron staining. Neither I nor Eren are familiar with a particular chert variety that is visually consistent with this material. Cantin’s (2008) descriptions of Kenneth and West Franklin chert might both describe this particular material but so too might some lighter-toned varieties of Onondaga chert (e.g., Jarvis 1988) that I have experience working with. Unfortunately, the MURR NAA database does not have representative samples of any of these materials, so it is currently not possible to compare the Mielke #1 artifacts to the source profiles of these particular cherts. Regardless, these artifacts form a cohesive group in bivariate and multivariate space, suggesting that they all likely derive from the same source. In nearly every respect, these samples overlap with the Upper Mercer source group; however, the coloration and luster of these artifacts make them quite distinct from Upper Mercer chert. Thus, even if the source of these artifacts is eventually discovered, visual characteristics will be required to distinguish them from Upper Mercer chert.

The final two artifacts from Mielke #1 (CHR356 and -357) are made on what appears to be chert from the Paoli Limestone of Indiana and Kentucky, locally referred to as Carter Cave flint. The MURR chert database does not presently contain any source samples of this material. The only previously analyzed pieces of suspected Paoli chert are artifacts analyzed as part of a 2018 study for Joseph Gingerich (Boulanger 2018). In that study, the Paoli chert specimens did not form a compositionally distinct group that could easily be distinguished from other Mississippian-aged cherts in the Midwest and Southeast. When compared against the current sampling of cherts from Ohio and elsewhere in the upper Midwest, specimen CHR356 consistently falls within the 90% confidence ellipse defined by the sample of artifacts that Gingerich visually identified as Paoli. Specimen CHR357 is far outside this same confidence interval and is generally characterized by extremely low values of most elements detected by NAA. This depletion in elements makes it compositionally similar to Burlington chert, Flint Ridge White, and some varieties of Upper Mercer chert. Visually, however, sample CHR357 is distinct from these chert types in its coloration and luster. These results suggest that (1) there are two somewhat chemically distinctive varieties of Paoli chert; (2) there are two chemically distinct cherts that are being visually classified as Paoli chert; or (3) the current sample of artifacts being used as a proxy for the chemical signature of Paoli chert does not adequately represent the entire range of elemental compositions present in this material.

A canonical discriminant analysis (CDA) of the chert-source groups discussed herein demonstrates that 74% of the cumulative variation between these groups can be represented by two discriminant functions. Projecting the Mielke #1 artifacts into this multivariate space (Figures 15–20) further shows their relationships to these groups. Artifacts identified as Harrodsburg (or Allens Creek) chert plot outside the 90% confidence ellipse representing the Harrodsburg source sample (see Figure 15). Yet, they also appear to form a distinct cluster themselves—again, demonstrating their internal geochemical similarities. Figure 16 shows the artifacts classified as Upper Mercer chert projected into this discriminant function. Specimens CHR306, -308, -312, and -314 all plot within the 90% confidence ellipse defined by Upper Mercer source samples from Coshocton County, Ohio. CHR307, -309, -311, and -313 fall outside this confidence interval. As discussed above, however, in other plots of these data, and in their visual characteristics, these samples all seem consistent with Upper Mercer chert from either

Coshocton County or Hocking County. One of these specimens (CHR309) exhibits visual characteristics that I believe make it a better match for Holland chert, and in CDA space, it does plot on the cusp of the 90% confidence interval for this source. Taking a conservative approach to interpreting these results, I would suggest that CHR309 is *either* Upper Mercer *or* Holland chert. Above, based on visual criteria alone, I would classify CHR310 as Wyandotte chert, and examination of the elemental and PCA data supports this classification. In CDA space, CHR310 also plots within the 90% confidence ellipse for the Wyandotte source sample. I would thus recommend that this is the most likely source for this particular artifact.

The CDA plot for artifacts visually classified as Flint Ridge chert (see Figure 17) also supports the conclusions offered above. Specimens CHR316, -319, -320, and -321, which I would describe as the white or chalcedonic variety of Flint Ridge chert, all plot within or adjacent to the compositional group represented by source specimens of this chert variety. Specimen CHR322, which is consistent with the primary variety of Flint Ridge chert, plots within the 90% confidence ellipse made of samples from the primary Flint Ridge quarries. In CDA space, specimen CHR315 plots within the 90% confidence interval of Burlington chert. This is consistent with how I would visually classify this particular artifact. As noted above, plotting these same data in bivariate elemental plots does not result in an unequivocal association of CHR315 with the Burlington source sample. However, the CDA plot appears to do so. Specimen CHR317, which both Eren and I would tentatively classify as Flint Ridge, plots well outside the 90% confidence ellipses for both the main Flint Ridge source and the Flint Ridge White variety. This appears to be because this particular sample has extremely low concentrations of nearly all elements detected by NAA. In other words, this piece is almost pure SiO_2. Because of these low concentrations of elements, in several cases below the detection limits of the procedures used here, CHR317 cannot always be plotted in elemental space. Although visually this piece would be identified as Flint Ridge chert, the geochemical data simply cannot be used to associate this sample with either variety of this material.

In Figure 18, the artifacts tentatively identified as Wyandotte chert are shown projected against source groups in CDA space. As discussed above, these artifacts split into two clear groupings: one compositionally similar to Wyandotte chert source samples and the other similar to the Upper Mercer and Flint Ridge samples. CHR332, which above I identified as likely belonging to the Nethers Farm (pinstripe) variety of Flint Ridge chert, plots within the 90% confidence interval of the primary Flint Ridge source sample, further supporting its association with this material. Specimens CHR333, -335, -336, -337, -338, -339, and -340 all fall within or adjacent to the Upper Mercer and Flint Ridge samples in CDA space, but they cannot be confidently associated with a specific source based solely on these data without reliance on their visual characteristics—which as noted previously are only consistent with the blue variety of Upper Mercer chert. The remaining artifacts identified as Wyandotte chert are geochemically consistent with source samples of this material, though CHR325 may be an exception as it tends to plot on the edge of or outside the Wyandotte source sample. Of note, the Wyandotte chert can be easily distinguished from Holland chert (potentially a visual look-alike), and none of the Mielke #1 artifacts exhibits compositions similar to the Holland source sample.

In multivariate CDA space, all the artifacts described as being gray/white chert plot on the margins of or outside the 90% confidence ellipses for nearly all the sources discussed herein (see Figure 19). Given these specimens' visual differences from all other cherts discussed here, this result is not entirely unsurprising. As noted above, while the geochemical data for these specimens cannot at present identify the source of this chert, it is possible to say that they are a geochemically and visually distinctive chert variety at Mielke #1.

Lastly, data for the Paoli (Carter Cave) chert specimens analyzed here remain somewhat equivocal. In CDA space (see Figure 20), specimen CHR357 plots well outside all compositional groups and other artifacts, while CHR356 falls closer to the Wyandotte and Hopkinsville source samples. While I agree with Eren's assessment that these two pieces are visually consistent with Paoli chert, it is important to reiterate that no sources of this material have been sampled by NAA at MURR.

As a final examination of these data, I calculated the Mahalanobis distance–based group-membership probabilities of the Mielke #1 artifacts for the largest chert-source groups in the current data set: Burlington, Flint Ridge, Upper Mercer, and Wyandotte. The small size of the remaining chert-source groups precludes their use in this procedure. Membership probabilities were calculated based on the first five principal components derived from the entire data set, accounting for 87.4% of the cumulative variance. The results (Table 5) suggest that the group assignments made from elemental bivariate plots and multidimensional plots in PCA and CDA space are robust; though, given how some of these groups overlap in compositional space, the highest probability of group membership does not always correspond to how I have chosen to classify specimens.

Conclusions

A summary of the source assignments for the Mielke #1 artifacts is provided in Table 6, along with the visually based assignments made by Eren and me. The results of the NAA on these artifacts strongly suggest that the presence of multiple lithic materials at the site, including Wyandotte, Upper Mercer, Flint Ridge, either Harrodsburg or Allens Creek, and Burlington chert. Some of these materials (e.g., Burlington and Upper Mercer) derive from sources at significant distance from the Mielke #1 site, though others represent sources less farther afield (e.g., Wyandotte, Harrodsburg/Allens Creek).

Results of this study show that nondestructive XRF may be of limited use for midwestern-chert sourcing studies. Nearly all elements measured here were at or below detection limits, regardless of the visual characteristics of the chert. The NAA data reported here reveal that elements that are useful for geochemically distinguishing source groups are present in these cherts in abundances less than 10 ppm—with most elements being present in trace (<1 ppm) amounts. It is, of course, possible to lower the detection limits of our calibration by increasing the counting time on the spectrometer. But it is unlikely that extended count times would resolve concentrations below 1 ppm given current technologies and the methods used here. Given the current capabilities of handheld XRF spectrometers in quantifying many elements at or below these levels, it seems reasonable to conclude that these instruments will be of limited use for characterizing the chert sources discussed here. Whether this same technique will be suitable for other chert sources has yet to be demonstrated.

Looking ahead to further lithic-source research, a more systematic sampling of some of the sources represented here is greatly needed. It would also be worth the effort to sample some of the materials for which only artifacts have been analyzed (e.g., Paoli chert). However, the results presented here suggest that continued efforts to employ geochemical analyses to establish the provenance of midwestern cherts have merit. Though, as admonished by Luedtke (1992), such efforts should involve systematic survey and sampling of chert sources and include other modes of analysis, such as megascopic, macroscopic, and microscopic studies, identification of minerals and microfossils, and consultation with available geological literature.

Acknowledgments

Support for this study was provided by the MURR Archaeometry Laboratory's NSF grant (#1912776), and I thank Dr. Michael Glascock and Dr. Brandi MacDonald of the laboratory for their support and assistance in conducting the NAA.

References

Bassett, John, and Richard L. Powell (1984) Stratigraphic Distribution of Cherts in Limestones of the Blue River Group in Southern Indiana. In *Prehistoric Chert Exploitation: Studies from the Midcontinent,* edited by Brian M. Butler and Ernest E. May, pp. 239–252. Center for Archaeological Investigations, Occasional Paper 2. Southern Illinois University, Carbondale.

Baxter, Mike J. (1992) Archaeological Uses of the Biplot—A Neglected Technique? In *Computer Applications and Quantitative Methods in Archaeology, 1991*, edited by Gary Lock and Jonathan Moffett, pp. 141–148. BAR International Series, Vol. S577. Tempus Reparatum, Oxford.

Baxter, Mike J. (1994) *Exploratory Multivariate Analysis in Archaeology*. Edinburgh University Press, Edinburgh, United Kingdom.

Baxter, Mike J., and Caitlin E. Buck (2000) Data Handling and Statistical Analysis. In *Modern Analytical Methods in Art and Archaeology*, edited by Enrico Ciliberto and Giuseppe Spoto, pp. 681–746. John Wiley and Sons, New York.

Bieber, A. M. J., D. W. Brooks, G. Harbottle, and E. V. Sayre (1976) Application of Multivariate Techniques to Analytical Data on Aegean Ceramics. *Archaeometry* 18:59–74.

Bishop, Ronald L., and Hector Neff (1989) Compositional Data Analysis in Archaeology. In *Archaeological Chemistry IV*, edited by Ralph O. Allen, pp. 576–586. Advances in Chemistry, Vol. 220. American Chemical Society, Washington, DC.

Bishop, Ronald L., Robert L. Rands, and George R. Holley (1982) Ceramic Compositional Analysis in Archaeological Perspective. *Advances in Archaeological Method and Theory* 5:275–330.

Boulanger, Matthew T. (2018) Chemical Characterization of Cryptocrystalline Silicates from Sources in the U.S. Southeast and from Smith Mountain (44PY152), Pittsylvania County, Virginia. Prepared for J. A. M. Gingerich, Smithsonian Institution, Washington, DC, by Matthew T. Boulanger, Southern Methodist University, Dallas, Texas.

Boulanger, Matthew T. (2019) Neutron Activation Analysis of Chert Sources in the Upper Midwest, and a Comparison to Bifaces from a Suspected Paleoindian Cache at Camp Cornish, Ohio. Prepared for MURR Archaeometry Laboratory, University of Missouri, Columbia, by Matthew T. Boulanger, Southern Methodist University, Dallas, Texas.

Boulanger, Mattherw T., Briggs Buchanan, Michael J. O'Brien, Brian G. Redmond, Michael D. Glascock, and Metin I. Eren (2015) Neutron Activation Analysis of 12,900-Year-Old Stone Artifacts Confirms 450–510+ km Clovis Tool-Stone Acquisition at Paleo

Crossing (33ME274), Northeast Ohio, U.S.A. *Journal of Archaeological Science* 53:550–558.

Boulanger, Matthew T., and W. D. Stoner (2012) Data Management and Sharing Plan (v. 1). Electronic document, https://archaeometry.missouri.edu/data_management.html, accessed April 22, 2022.

Cantin, M. (1994) Provenience, Description, and Archaeological Use of Selected Cherts in Indiana. Manuscript on file, Indiana State University, Terre Haute.

Cantin, M. (2008) Provenience, Description, and Archaeological Use of Selected Cherts in Indiana. Technical Report 05-01. Indiana State University Anthropology Laboratory, Terre Haute, Indiana.

Carlson, Ernest H. (1987) Flint Ridge, Ohio: Flint Facies of the Pennsylvanian Vanport Limestone. In *Centennial Field Guide 3*, edited by Donald L. Biggs, pp. 415–418. North-Central Section of the Geological Society of America, Boulder, Colorado.

Carlson, Ernest H. (1991) *Minerals of Ohio.* Bulletin 69. Ohio Division of Geological Survey, Columbus.

Chiarulli, Beverly, and Gregory Katz (2016) Chert Sourcing Studies in Western and Central Pennsylvania. Paper presented at the Pennsylvania Archaeological Council Symposium, Annual Meeting of the Society for Pennsylvania Archaeology, West Middlesex, Pennsylvania.

Converse, R. N. (2007) *Ohio Flint Types.* Archaeological Society of Ohio, Columbus.

DeRegnaucourt, Tony, and Jeff A. Georgiady (1998) *Prehistoric Chert Types of the Midwest.* Western Ohio Podiatric Medical Center, Greenville, Ohio.

Georgiady, Jeff A., and Mark E. Brockmann (2002) *Prehistoric Lithic Types of New England.* Franklin Printing, Farmington, Maine.

Glascock, Michael D. (1992) Characterization of Archaeological Ceramics at MURR by Neutron Activation Analysis and Multivariate Statistics. In *Chemical Characterization of Ceramic Pastes in Archaeology*, edited by Hector Neff, pp. 11–26. Prehistory Press, Madison, Wisconsin.

Glascock, Michael D. (2004) Neutron Activation Analysis of Chert Artifacts from a Hopewell Mound. *Journal of Radioanalytical and Nuclear Chemistry* 262:91–102.

Glascock, Michael D., and Jeffrey R. Ferguson (2012) Report on the Analysis of Obsidian Source Samples by Multiple Analytical Methods. Prepared for Bruker, Kennewick, Washington, by Archaeometry Laboratory, University of Missouri Research Reactor, Columbia.

Glascock, Michael D., and Hector Neff (2003) Neutron Activation Analysis and Provenance Research in Archaeology. *Measurement Science and Technology* 14:1516–1526.

Harbottle, G. (1976) Activation Analysis in Archaeology. *Radiochemistry* 3(1):33–72.

Ives, David J. (1975) *The Crescent Hills Prehistoric Quarrying Area*. Museum Briefs 22. Museum of Anthropology, University of Missouri, Columbia.

Jarvis, H. (1988) INAA Characterization of Onondaga Chert: A Preliminary Study in Western New York. Master's thesis, Department of Anthropology, State University of New York at Buffalo.

Leese, M. N., and Peter L. Main (1994) The Efficient Computation of Unbiased Mahalanobis Distances and Their Interpretation in Archaeometry. *Archaeometry* 36:307–316.

Lepper, Bradley T., Richard W. Yerkes, and William H. Pickard (2001) Prehistoric Flint Procurement Strategies at Flint Ridge, Licking County, Ohio. *Midcontinental Journal of Archaeology* 26:53–78.

Limpert, Eckhard, Werner A. Stahel, and Markus Abbt (2001) Log-Normal Distributions across the Sciences: Keys and Clues. *Bioscience* 51(5):341–352.

Luedtke, Barbara E. (1976) Lithic Material Distributions and Interaction Patterns during the Late Woodland Period in Michigan, 2 vols. PhD dissertation, Department of Anthropology, University of Michigan, Ann Arbor.

Luedtke, Barbara E. (1992) *An Archaeologist's Guide to Chert and Flint*. Archaeological Research Tools 7. Cotsen Institute of Archaeology, University of California, Los Angeles.

Morrow, Carol A., J. Michael Elam, and Michael D. Glascock (1992) The Use of Blue-Grey Chert in Midwestern Prehistory: The Need for Baseline Data. *Midcontinental Journal of Archaeology* 17:166–197.

Murphy, James L., and John E. Blank (1970) The Plum Run Flint Quarries. *Ohio Archaeologist* 20(2):197–200, 217.

Neff, Hector (1994) RQ-mode Principal Component Analysis of Ceramic Compositional Data. *Archaeometry* 36:115–130.

Neff, Hector (2000) Neutron Activation Analysis for Provenance Determination in Archaeology. In *Modern Analytical Methods in Art and Archaeology*, edited by Enrico Ciliberto and Giuseppe Spoto, pp. 81–134. John Wiley and Sons, New York.

Neff, Hector (2002) Quantitative Techniques for Analyzing Ceramic Compositional Data. In *Ceramic Source Determination in the Greater Southwest*, edited by Donna M. Glowacki and Hector Neff, pp. 15–36. Monograph 44. Cotsen Institute of Archaeology, Los Angeles.

Palarea-Albaladejo, Javier, and Josep Antoni Martín-Fernández (2015) zCompositions—R Package for Multivariate Imputation of Left-Censored Data under a Compositional Approach. *Chemometrics and Intelligent Laboratory Systems* 143:85–96.

Palarea-Albaladejo, Javier, Josep Antoni Martín-Fernández, and Ricardo Antonio Olea (2014) A Bootstrap Estimation Scheme for Chemical Compositional Data With Nondetects. *Journal of Chemometrics* 28:585–599.

Speakman, Robert J. (2012) Evaluation of Bruker's Tracer Family Factory Obsidian Calibration for Handheld Portable XRF Studies of Obsidian. Prepared for Bruker, Kennewick, Washington, by Center for Applied Isotope Studies, University of Georgia, Athens.

Stout, Wilbur, and R. A. Schoenlaub (1946) *The Occurrence of Flint in Ohio.* Bulletin 46. Department of Natural Resources, Division of Geological Survey, Columbus.

Tankersley, Kenneth B. (1985) Mineralogical Properties of Wyandotte Chert as an Aid to Archaeological Fingerprinting. In *Lithic Resource Procurement: Proceedings from the Second Conference on Prehistoric Chert Exploitation*, edited by Susan C. Vehik, pp. 251–264. Center for Archaeological Investigations, Southern Illinois University at Carbondale.

Tankersley, Kenneth B. (1989) Late Pleistocene Lithic Exploitation and Human Settlement in the Midwestern United States. PhD dissertation, Department of Anthropology, Indiana University, Bloomington.

Weigand, Phil C., Garman Harbottle, and Edward V. Sayre (1977) Turquoise Sources and Source Analysis: Mesoamerica and the Southwestern U.S.A. In *Exchange Systems in Prehistory*, edited by Timothy K. Earle and Jonathon E. Ericson, pp. 15–34. Academic Press, New York.

White, Andrew A. (2002) Survey and Excavations in the Nugent East Area, Clark County, Indiana, 1998–1999. Reports of Investigations 206. Prepared for Nugent Sand Company by Indiana University–Purdue University at Fort Way Archaeological Survey.

Table 1. Analytical Results of the RGM-1 Check-Standard Used at SMU for XRF Analyses (Average of 4 Assays) Compared to USGS and GeoRem Preferred Values.

	Ti	Mn	Fe %	Zn	Ga	Rb	Sr	Y	Zr	Nb	Ba	Th
RGM-1	1509	295	1.317	33.5	15.5	152	112	20.5	236.5	8.5	810	14
USGS	1618	280	1.301	32		150	110	25	220	8.9	810	15
GeoRem	1591	300	1.309	33	16	150	105	23	228	9	827	15

Note: All values in parts per million unless otherwise noted.

Table 2. Abundances for 12 Elements Determined by Nondestructive XRF at SMU.

ANID	Ti	Mn	Fe%	Zn	Ga	Rb	Sr	Y	Zr	Nb	Ba	Th
MIELKE0001	<LOD	<LOD	0.182	6	<LOD	<LOD	5	4	<LOD	<LOD	<LOD	<LOD
MIELKE0002	<LOD	<LOD	0.089	9	<LOD	<LOD	10	5	<LOD	<LOD	<LOD	<LOD
MIELKE0003	258	66	0.150	<LOD	<LOD	<LOD	9	5	<LOD	<LOD	29	<LOD
MIELKE0004	<LOD	<LOD	0.043	<LOD	<LOD	<LOD	13	3	<LOD	<LOD	<LOD	<LOD
MIELKE0005	<LOD	<LOD	0.040	<LOD	<LOD	<LOD	<LOD	4	<LOD	<LOD	<LOD	<LOD
MIELKE0008	<LOD	<LOD	0.129	<LOD	<LOD	<LOD	17	4	<LOD	<LOD	<LOD	L<OD
MIELKE0009	<LOD	<LOD	0.068	<LOD	<LOD	<LOD	6	3	<LOD	<LOD	<LOD	<LOD
MIELKE0010	131	<LOD	0.064	<LOD	<LOD	<LOD	11	4	<LOD	<LOD	<LOD	<LOD
MIELKE0011	<LOD	<LOD	0.107	<LOD	<LOD	<LOD	71	4	46	<LOD	<LOD	<LOD
MIELKE0013	344	347	1.417	33	<LOD	<LOD	4	9	<LOD	<LOD	<LOD	<LOD
MIELKE0014	<LOD	<LOD	0.126	<LOD	<LOD	<LOD	6	4	<LOD	<LOD	<LOD	<LOD
MIELKE0015	93	<LOD	0.082	17	<LOD	<LOD	22	3	<LOD	<LOD	<LOD	<LOD
MIELKE0016	<LOD	<LOD	0.171	<LOD	<LOD	<LOD	18	4	<LOD	<LOD	<LOD	<LOD
MIELKE0017	<LOD	<LOD	0.128	8	<LOD	<LOD	20	3	<LOD	<LOD	<LOD	<LOD
MIELKE0018	<LOD	<LOD	0.102	<LOD	<LOD	<LOD	7	3	<LOD	<LOD	<LOD	<LOD
MIELKE0019	128	<LOD	0.183	28	<LOD	<LOD	7	4	<LOD	<LOD	<LOD	<LOD
MIELKE0020	94	<LOD	0.093	<LOD	<LOD	<LOD	149	2	10	<LOD	<LOD	<LOD
MIELKE0021	<LOD	<LOD	0.167	<LOD	<LOD	<LOD	9	4	<LOD	L<OD	<LOD	<LOD
MIELKE0022	144	<LOD	0.153	<LOD	<LOD	<LOD	8	4	<LOD	<LOD	<LOD	<LOD
MIELKE0023	132	26	0.394	<LOD	<LOD	<LOD	3	4	<LOD	<LOD	<LOD	<LOD
MIELKE0024	<LOD	110	0.096	<LOD	<LOD	<LOD	6	4	<LOD	<LOD	<LOD	<LOD
MIELKE0025	631	120	0.891	6	<LOD	6	13	5	5	<LOD	<LOD	<LOD

MIELKE0026	149	48	1.281	5	<LOD	<LOD	38	5	<LOD	<LOD	<LOD	<LOD
MIELKE0027	<LOD	<LOD	0.037	<LOD	<LOD	<LOD	1	4	<LOD	<LOD	<LOD	<LOD
MIELKE0028	<LOD	<LOD	0.076	17	<LOD	<LOD	14	4	<LOD	<LOD	<LOD	<LOD
MIELKE0312	249	<LOD	0.518	<LOD	<LOD	<LOD	54	6	3	<LOD	98	<LOD
MIELKE0313	342	69	0.702	6	<LOD	<LOD	29	4	<LOD	<LOD	26	<LOD
MIELKE0318	179	<LOD	0.088	<LOD	<LOD	<LOD	30	20	3	1	86	<LOD
MIELKE0319	352	64	0.323	<LOD	<LOD	<LOD	7	6	59	<LOD	<LOD	<LOD
MIELKE0333	189	<LOD	0.419	<LOD	<LOD	<LOD	24	3	2	<LOD	306	<LOD
MIELKE0443	<LOD	<LOD	0.057	<LOD	<LOD	<LOD	2	3	<LOD	<LOD	<LOD	<LOD
MIELKE0007	<LOD	<LOD	0.111	<LOD	<LOD	<LOD	13	4	<LOD	<LOD	<LOD	<LOD
MIELKE0006	<LOD	<LOD	0.038	<LOD	<LOD	<LOD	<LOD	3	<LOD	<LOD	<LOD	<LOD
MIELKE0012	<LOD	<LOD	0.058	<LOD	<LOD	<LOD	19	3	<LOD	<LOD	<LOD	<LOD
MIELKE0296	<LOD	<LOD	0.130	<LOD	<LOD	<LOD	5	4	<LOD	<LOD	<LOD	<LOD
MIELKE0297	190	29	1.960	16	<LOD	<LOD	17	5	<LOD	<LOD	79	<LOD
MIELKE0299	263	<LOD	0.166	<LOD	<LOD	<LOD	17	5	<LOD	<LOD	115	<LOD
MIELKE0300	<LOD	<LOD	0.453	<LOD	<LOD	<LOD	5	4	<LOD	<LOD	<LOD	<LOD
MIELKE0304	<LOD	<LOD	0.060	<LOD	<LOD	<LOD	<LOD	4	<LOD	<LOD	<LOD	<LOD

Note: All elements in parts per million unless otherwise noted.
<LOD indicates values are lower than detection limits for the calibration.

Table 3. Analytical Identifier (ANID), Sample Number, Mass, and Description of Chert Samples from Mielke #1.

ANID	Sample	Mass (g)	Description	MIE ID	MTB ID
CHR296	1	8.7	Retouched flake	Harrodsburg	Allens Creek / Harrodsburg
CHR297	2	15	Overshot flake	Harrodsburg	Allens Creek / Harrodsburg
CHR298	3	18.2	Retouched flake	Harrodsburg	Allens Creek / Harrodsburg
CHR299	4	3.4	Flake	Harrodsburg	Allens Creek / Harrodsburg
CHR300	5	5.5	Flake	Harrodsburg	Allens Creek / Harrodsburg
CHR301	6	2.7	Flake	Harrodsburg	Allens Creek / Harrodsburg
CHR302	7	1.3	Flake	Harrodsburg	Allens Creek / Harrodsburg
CHR303	8	0.8	Flake	Harrodsburg	Allens Creek / Harrodsburg
CHR304	9	2	Flake	Harrodsburg	Allens Creek / Harrodsburg
CHR305	10	1.8	Retouched flake	Harrodsburg	Allens Creek / Harrodsburg
CHR306	11	15.9	Biface	Upper Mercer	Upper Mercer: Bird-Dropping
CHR307	12	14.8	Biface tip	Upper Mercer	Upper Mercer: Coshocton Gray
CHR308	13	11.2	Retouched flake	Upper Mercer	Upper Mercer: Blue
CHR309	14	11.6	Retouched flake	Upper Mercer	Wyandotte / Holland
CHR310	15	7.4	Retouched flake	Upper Mercer	Wyandotte / Holland
CHR311	16	8.5	Bipolar core	Upper Mercer	Coshocton Black
CHR312	17	2.2	Flake	Upper Mercer	Coshocton Black
CHR313	18	1	Flake	Upper Mercer	Coshocton Black
CHR314	19	1	Flake	Upper Mercer	Wyandotte / Holland
CHR315	20	7.5	End scraper	Flint Ridge	Burlington (Heat treated)
CHR316	21	8.6	Biface	Flint Ridge	Flint Ridge
CHR317	22	3.4	End scraper	Flint Ridge	Flint Ridge?
CHR318	23	3.6	Platform rejuv. flake	Flint Ridge	Flint Ridge: White
CHR319	24	2.1	Retouched flake	Flint Ridge	Flint Ridge: White
CHR320	25	2.4	Biface	Flint Ridge	Flint Ridge
CHR321	26	1.3	Flake	Flint Ridge	Flint Ridge
CHR322	27	1.2	Flake	Flint Ridge	Flint Ridge
CHR323	28	9.4	Flake	Wyandotte	Wyandotte
CHR324	29	12	End scraper	Wyandotte	Wyandotte
CHR325	30	11.4	Scraper	Wyandotte	Wyandotte

CHR326	31	7.1	Scraper	Wyandotte	Wyandotte
CHR327	32	4.3	Bladelet	Wyandotte	Wyandotte
CHR328	33	5.1	Retouched flake	Wyandotte	Wyandotte
CHR329	34	5.4	Scraper	Wyandotte	Wyandotte
CHR330	35	4.6	Blockshatter	Wyandotte	Holland
CHR331	36	2.1	Retouched flake	Wyandotte	
CHR332	37	0.9	Flake	Wyandotte	Flint Ridge: Pinstripe
CHR333	38	1.1	Blockshatter	Wyandotte	
CHR334	39	0.7	Flake	Wyandotte	
CHR335	40	8.2	Retouched flake	Wyandotte	
CHR336	41	5.7	Blockshatter	Wyandotte	Holland: Dark Phase
CHR337	42	4.9	Blockshatter	Wyandotte	
CHR338	43	1.9	Blockshatter	Wyandotte	
CHR339	44	0.8	Flake	Wyandotte	
CHR340	45	1.3	Flake	Wyandotte	

Table 3, continued.

ANID	Sample	Mass (g)	Description	MIE ID	MTB ID
CHR341	46	20.8	Poplar Island Point	Gray/White w/iron	
CHR342	47	7.1	Blockshatter	Gray/White w/iron	
CHR343	48	10.4	Overshot flake	Gray/White w/iron	
CHR344	49	10.4	Biface	Gray/White w/iron	
CHR345	50	2.8	Blockshatter	Gray/White w/iron	
CHR346	51	3.4	Lamok Pointa	Gray/White w/iron	
CHR347	52	5.1	End scraper	Gray/White w/iron	
CHR348	53	1.9	Blockshatter	Gray/White w/iron	
CHR349	54	2.1	Blockshatter	Gray/White w/iron	
CHR350	55	2.3	Blockshatter	Gray/White w/iron	
CHR351	56	1.7	Retouched flake	Gray/White w/iron	
CHR352	57	1.7	Blockshatter	Gray/White w/iron	

CHR353	58	2.2	Potlid	Gray/White w/iron	
CHR354	59	1.1	Flake	Gray/White w/iron	
CHR355	60	0.4	Flake	Gray/White w/iron	
CHR356	61	17.9	Retouched flake	Carters Cave	Paoli
CHR357	62	14.9	Flake	Carters Cave	Paoli

Table 4. The First Eight Components of a Principal Components Analysis, Explaining 91.54% of the Cumulative Variance in the Data Set.

	PC1	**PC2**	**PC3**	**PC4**	**PC5**	**PC6**	**PC7**	**PC8**
Variance	56.42	13.01	7.30	5.15	3.28	2.55	2.16	1.66
Cum. Variance	56.42	69.44	76.74	81.89	85.17	87.72	89.88	91.54
Eigenvector	3.95	0.91	0.51	0.36	0.23	0.18	0.15	0.12
Al	**0.071**	-0.075	0.012	-0.022	0.057	0.034	0.096	0.120
As	**0.078**	**-0.150**	-0.011	0.109	**-0.344**	**-0.366**	-0.035	**0.495**
Ba	0.197	-0.019	0.120	-0.150	0.218	**-0.326**	**0.707**	0.265
Ca	0.188	-0.048	**-0.210**	**0.344**	0.190	**0.571**	0.105	0.251
Ce	0.251	0.056	0.129	-0.057	0.139	-0.113	0.045	-0.167
Co	0.203	**-0.260**	-0.033	0.175	**-0.218**	-0.082	-0.238	-0.136
Cr	0.180	-0.119	-0.106	-0.198	-0.063	0.058	-0.099	0.081
Cs	0.164	-0.083	**-0.131**	**-0.296**	0.017	0.001	-0.099	-0.040
Dy	**0.091**	0.080	**0.340**	0.150	-0.005	0.063	-0.013	0.199
Eu	0.170	-0.026	**0.373**	-0.062	-0.078	0.103	-0.183	-0.042
Fe	0.136	**-0.402**	0.013	0.211	-0.045	**-0.320**	-0.017	**-0.260**
Hf	0.210	0.017	**-0.274**	**-0.279**	0.123	0.036	-0.118	0.059
La	0.224	0.047	0.185	-0.067	0.086	-0.058	-0.095	-0.193
Lu	0.203	0.133	0.126	0.062	0.083	0.149	-0.083	0.291
Mn	0.170	**-0.440**	-0.062	**0.391**	**0.464**	-0.120	-0.161	0.092
Na	**0.092**	-0.051	-0.011	-0.061	-0.020	0.082	0.064	0.055
Nd	0.236	0.138	0.194	-0.025	0.082	-0.148	0.059	-0.138
Rb	0.165	-0.132	-0.105	**-0.257**	0.092	-0.015	-0.058	0.008
Sb	0.233	**0.290**	**-0.345**	0.213	**-0.456**	-0.188	-0.031	0.167
Sc	0.133	-0.105	-0.003	-0.207	-0.091	0.076	-0.086	0.214
Sm	0.271	**0.212**	0.129	0.071	-0.049	-0.068	-0.080	-0.189
Sr	0.213	0.057	**-0.219**	-0.131	0.011	0.031	0.065	-0.122
Ta	0.164	-0.071	-0.117	-0.196	0.066	0.037	-0.090	0.029
Tb	0.152	0.080	**0.367**	0.042	-0.109	0.108	-0.134	0.102
Th	0.152	-0.115	-0.024	**-0.290**	-0.034	0.047	-0.140	0.110
U	**0.338**	**0.398**	**-0.248**	**0.266**	0.114	-0.031	0.082	-0.216
Yb	0.152	0.069	0.253	-0.007	-0.011	0.090	-0.086	0.139
Zn	0.194	**-0.353**	0.066	0.026	**-0.455**	**0.390**	**0.469**	**-0.273**

Note: Significant loading is indicated in bold.

Table 5. Mahalanobis-Distance-Based Group-Membership Probabilities of the Mielke #1 Artifacts.

ANID	Burlington	Flint Ridge	Upper Mercer	Wyandotte
CHR296	**6.26084**	1.48863	3.85043	0.00022
CHR297	3.08682	**13.24249**	0.21188	0.00005
CHR298	6.75105	0.45158	**7.11277**	0.00018
CHR299	15.07991	0.83932	**59.84901**	0.00000
CHR300	7.78873	7.15389	**23.84223**	0.00274
CHR301	11.43242	0.85166	**55.89625**	0.00000
CHR302	10.16278	47.06865	**80.86586**	0.00006
CHR303	10.81929	1.13190	**12.84152**	0.00000
CHR304	7.24237	**7.72267**	1.12182	0.00050
CHR305	4.04114	1.59667	**32.35289**	0.00002
CHR306	0.75355	25.89951	**27.83724**	0.00468
CHR307	0.27433	**84.24477**	1.45009	0.00000
CHR308	6.02594	6.51161	**68.71780**	0.00003
CHR309	0.12821	**29.81538**	2.67788	0.07518
CHR310	0.00415	0.00006	0.00000	**3.08828**
CHR311	0.10479	**71.20540**	0.14114	0.00000
CHR312	4.48942	**4.98190**	3.04331	0.00000
CHR313	3.72952	**93.27204**	68.42769	0.00007
CHR314	1.98805	**90.09095**	71.89976	0.13961
CHR315	**64.52612**	0.68459	22.69410	0.00000
CHR316	16.57827	2.24289	**91.36693**	0.00000
CHR317	**2.92696**	0.83954	2.10518	0.00000
CHR318	6.24528	0.65177	**21.06558**	0.00000
CHR319	5.54741	**69.17478**	19.89431	0.00081
CHR320	11.79142	**17.01057**	2.79167	0.00000
CHR321	0.46669	**63.27411**	19.13948	0.00000
CHR322	2.24849	**65.14174**	14.67904	0.00012
CHR323	0.09846	1.02296	0.00541	**28.15279**
CHR324	0.03965	0.09127	0.00019	**91.82151**
CHR325	**0.12732**	0.05258	0.00019	0.01117
CHR326	0.05372	0.50116	0.00078	**89.88588**
CHR327	0.09664	0.47036	0.00101	**33.84248**
CHR328	0.04526	0.32064	0.00046	**40.60989**
CHR329	0.05876	1.20714	0.00382	**44.57743**
CHR330	3.80540	18.56997	**62.64090**	0.00077
CHR331	0.00905	0.00081	0.00000	**1.84509**
CHR332	20.62644	51.16947	**58.62935**	0.00000
CHR333	1.39339	**12.44990**	11.75013	0.00017

CHR334	0.05083	0.11853	0.00019	**8.99435**
CHR335	0.75211	**80.05792**	26.41978	0.02210

Note: Probabilities based on the first five PCs, accounting for 87.4% of the cumulative variance.

Table 5, continued.

ANID	Burlington	Flint Ridge	Upper Mercer	Wyandotte
CHR336	3.98483	57.25182	**77.71399**	0.00011
CHR337	13.88938	**23.45530**	8.66691	0.00000
CHR338	11.10903	20.16866	**69.03333**	0.00000
CHR339	0.42043	**92.80307**	9.38309	0.02671
CHR340	0.80580	**3.96561**	1.98195	0.00004
CHR341	1.16709	**97.03255**	25.29095	0.00024
CHR342	18.83675	8.17666	**90.40938**	0.00000
CHR343	34.90970	2.49416	**82.71696**	0.00000
CHR344	**72.93212**	0.24649	38.94446	0.00000
CHR345	2.89045	8.68079	**24.90788**	0.00001
CHR346	6.20578	1.98738	**38.90419**	0.00002
CHR347	1.74426	**85.95900**	65.64060	0.00000
CHR348	5.45843	20.26124	**54.79971**	0.00108
CHR349	24.44339	2.08624	**67.19520**	0.00000
CHR350	2.96595	14.85071	**52.88038**	0.00000
CHR351	2.13549	32.85273	**55.52272**	0.07927
CHR352	27.14120	2.40256	**67.14776**	0.00000
CHR353	24.42667	2.09844	**71.24886**	0.00000
CHR354	**15.88327**	1.38130	9.52950	0.00000
CHR355	11.62854	14.70431	**74.34633**	0.00000
CHR356	0.12479	**0.78316**	0.00530	0.24870
CHR357	**9.25764**	3.74012	5.87224	0.00000

Table 6. Analytical Identifier (ANID), Sample Number, Mass, and Description of Chert Samples from Mielke #1.

ANID	MIE ID	MTB ID	Source Assignment
CHR296	Harrodsburg	Allens Creek / Harrodsburg	Allens Creek / Harrodsburg?
CHR297	Harrodsburg	Allens Creek / Harrodsburg	Allens Creek / Harrodsburg?
CHR298	Harrodsburg	Allens Creek / Harrodsburg	Allens Creek / Harrodsburg?
CHR299	Harrodsburg	Allens Creek / Harrodsburg	Allens Creek / Harrodsburg?
CHR300	Harrodsburg	Allens Creek / Harrodsburg	Allens Creek / Harrodsburg?
CHR301	Harrodsburg	Allens Creek / Harrodsburg	Allens Creek / Harrodsburg?
CHR302	Harrodsburg	Allens Creek / Harrodsburg	Allens Creek / Harrodsburg?
CHR303	Harrodsburg	Allens Creek / Harrodsburg	Allens Creek / Harrodsburg?
CHR304	Harrodsburg	Allens Creek / Harrodsburg	Allens Creek / Harrodsburg?
CHR305	Harrodsburg	Allens Creek / Harrodsburg	Allens Creek / Harrodsburg?
CHR306	Upper Mercer	Upper Mercer: Bird-Dropping	Upper Mercer
CHR307	Upper Mercer	Upper Mercer: Coshocton Gray	cf. Upper Mercer
CHR308	Upper Mercer	Upper Mercer: Blue	Upper Mercer
CHR309	Upper Mercer	Wyandotte / Holland	Upper Mercer or Holland
CHR310	Upper Mercer	Wyandotte / Holland	Wyandotte
CHR311	Upper Mercer	Coshocton Black	cf. Upper Mercer
CHR312	Upper Mercer	Coshocton Black	Upper Mercer
CHR313	Upper Mercer	Coshocton Black	cf. Upper Mercer
CHR314	Upper Mercer	Wyandotte / Holland	Upper Mercer
CHR315	Flint Ridge	Burlington (Heat treated)	cf. Burlington
CHR316	Flint Ridge	Flint Ridge	Flint Ridge (cf. White)
CHR317	Flint Ridge	Flint Ridge?	Flint Ridge?
CHR318	Flint Ridge	Flint Ridge: White	Flint Ridge (cf. White)
CHR319	Flint Ridge	Flint Ridge: White	Flint Ridge: White
CHR320	Flint Ridge	Flint Ridge	Flint Ridge: White
CHR321	Flint Ridge	Flint Ridge	Flint Ridge: White
CHR322	Flint Ridge	Flint Ridge	Flint Ridge
CHR323	Wyandotte	Wyandotte	Wyandotte
CHR324	Wyandotte	Wyandotte	Wyandotte
CHR325	Wyandotte	Wyandotte	Wyandotte?

CHR326	Wyandotte	Wyandotte	Wyandotte
CHR327	Wyandotte	Wyandotte	Wyandotte
CHR328	Wyandotte	Wyandotte	Wyandotte
CHR329	Wyandotte	Wyandotte	Wyandotte
CHR330	Wyandotte	Holland	Wyandotte
CHR331	Wyandotte		
CHR332	Wyandotte	Flint Ridge: Pinstripe	Flint Ridge: Nethers Farm
CHR333	Wyandotte		Upper Mercer?
CHR334	Wyandotte		Wyandotte
CHR335	Wyandotte		Upper Mercer?
CHR336	Wyandotte	Holland: Dark Phase	Upper Mercer?
CHR337	Wyandotte		Upper Mercer?
CHR338	Wyandotte		Upper Mercer?
CHR339	Wyandotte		Upper Mercer?
CHR340	Wyandotte		Upper Mercer?

Table 6, continued.

ANID	MIE ID	MTB ID	Source Assignment
CHR341	Gray/White w/iron		Unidentified
CHR342	Gray/White w/iron		Unidentified
CHR343	Gray/White w/iron		Unidentified
CHR344	Gray/White w/iron		Unidentified
CHR345	Gray/White w/iron		Unidentified
CHR346	Gray/White w/iron		Unidentified
CHR347	Gray/White w/iron		Unidentified
CHR348	Gray/White w/iron		Unidentified
CHR349	Gray/White w/iron		Unidentified
CHR350	Gray/White w/iron		Unidentified
CHR351	Gray/White w/iron		Unidentified
CHR352	Gray/White w/iron		Unidentified
CHR353	Gray/White w/iron		Unidentified
CHR354	Gray/White w/iron		Unidentified
CHR355	Gray/White w/iron		Unidentified
CHR356	Carters Cave	Paoli/Carter Cave	Paoli?
CHR357	Carters Cave	Paoli/Carter Cave	Paoli?

Figure 1. Location of Mielke #1 (33SH26) in Shelby County, Ohio.

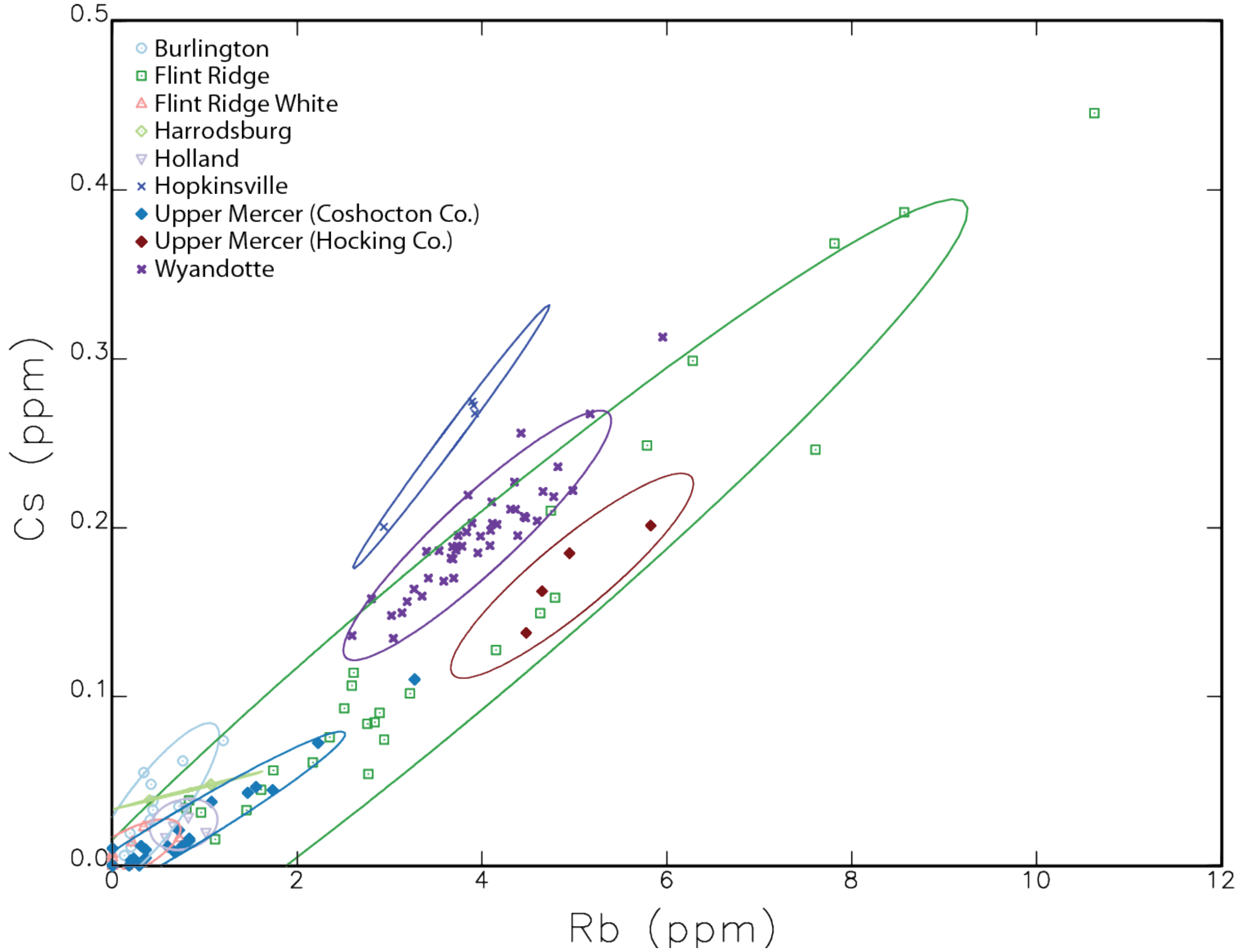

Figure 2. Bivariate plot of Cs and Rb showing chert sources discussed herein. Ellipses represent the 90% confidence interval of group membership.

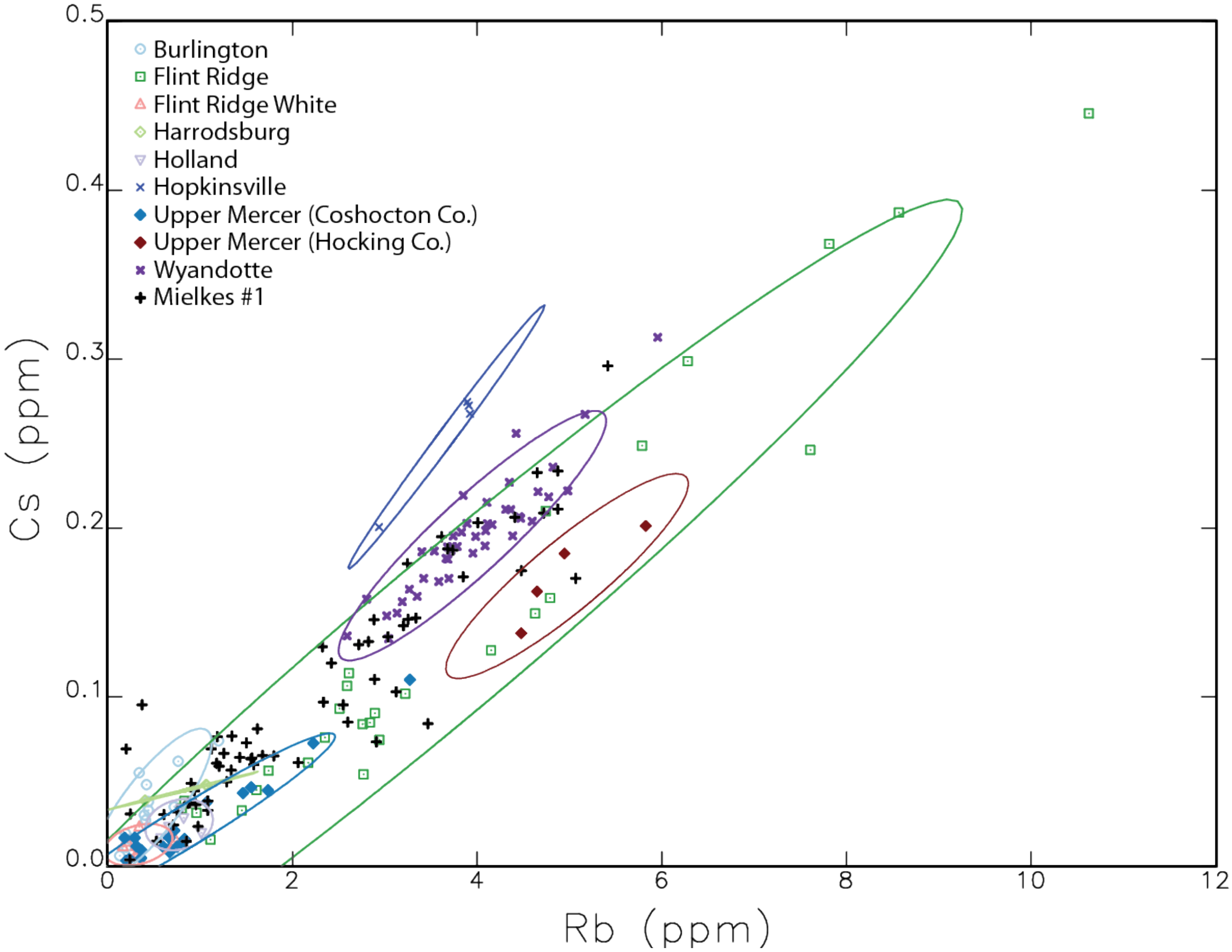

Figure 3. Bivariate plot of Cs and Rb showing chert sources and artifacts from Mielke #1. Ellipses represent the 90% confidence interval of group membership.

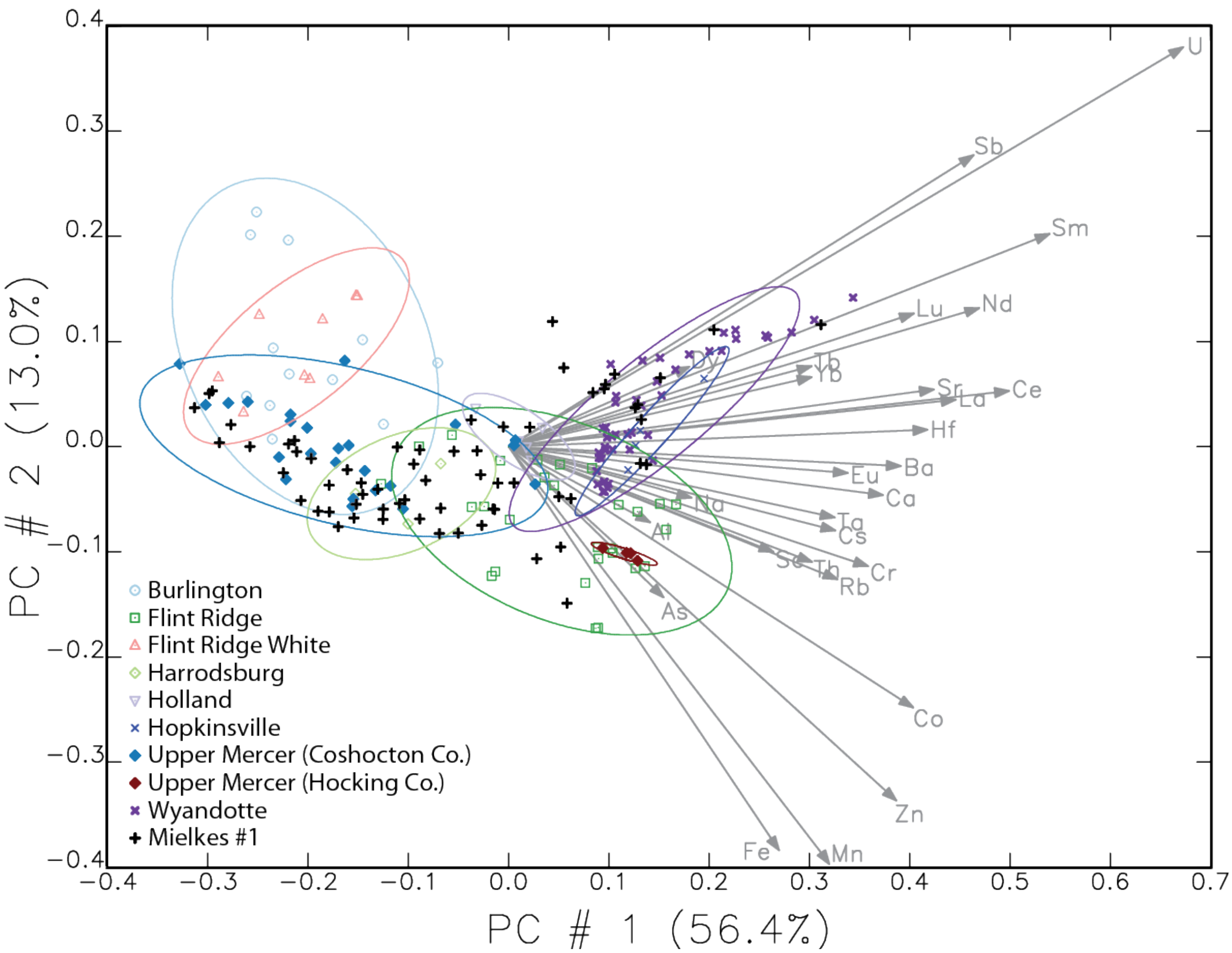

Figure 4. Principal components biplot of the first two components, accounting for 69.44% of the cumulative variance in the data.

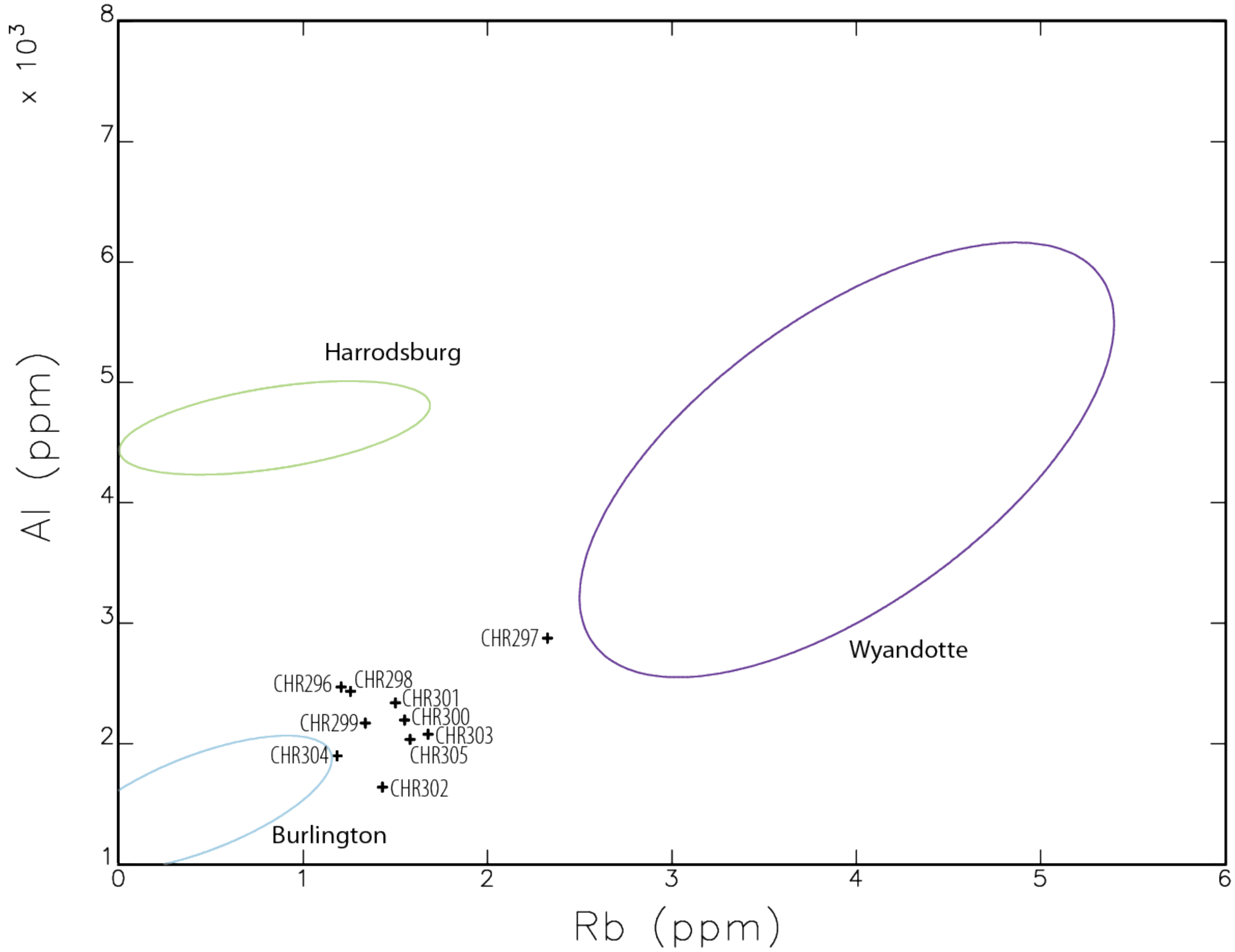

Figure 5. Bivariate plot of Al and Rb concentrations showing the Burlington, Harrodsburg, and Wyandotte compositional groups with 90% confidence ellipses, and the 10 Mielke #1 artifacts visually identified as Harrodsburg chert.

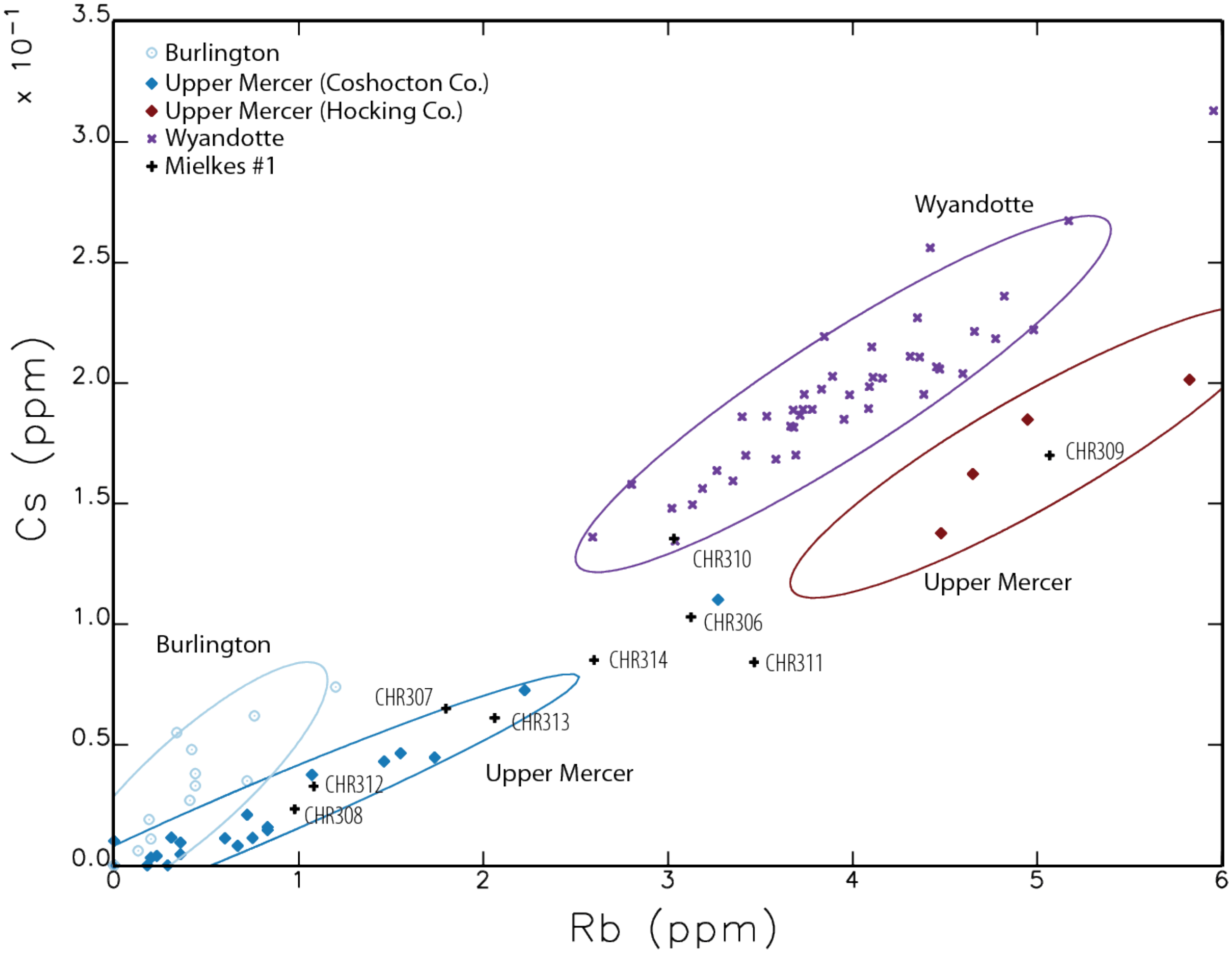

Figure 6. Bivariate plot of Cs and Rb showing Mielke #1 artifacts visually classified as Upper Mercer chert projected against source groups for Burlington, Upper Mercer, and Wyandotte cherts. Ellipses are plotted at the 90% confidence interval.

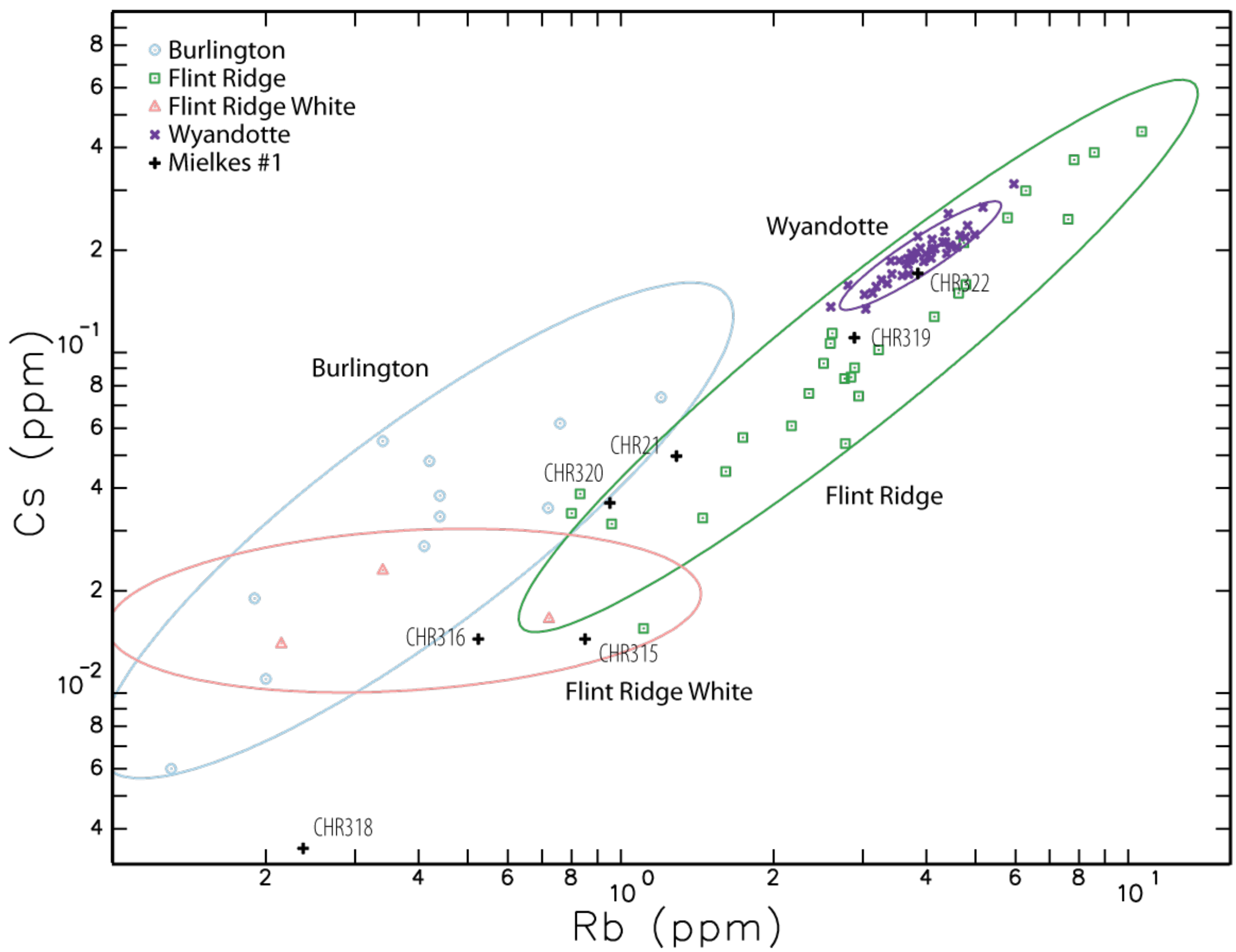

Figure 7. Bivariate plot of Cs and Rb showing Mielke #1 artifacts visually classified as Flint Ridge, plotted against source groups for Burlington, Flint Ridge, and Wyandotte cherts. Ellipses are plotted at the 90% confidence interval.

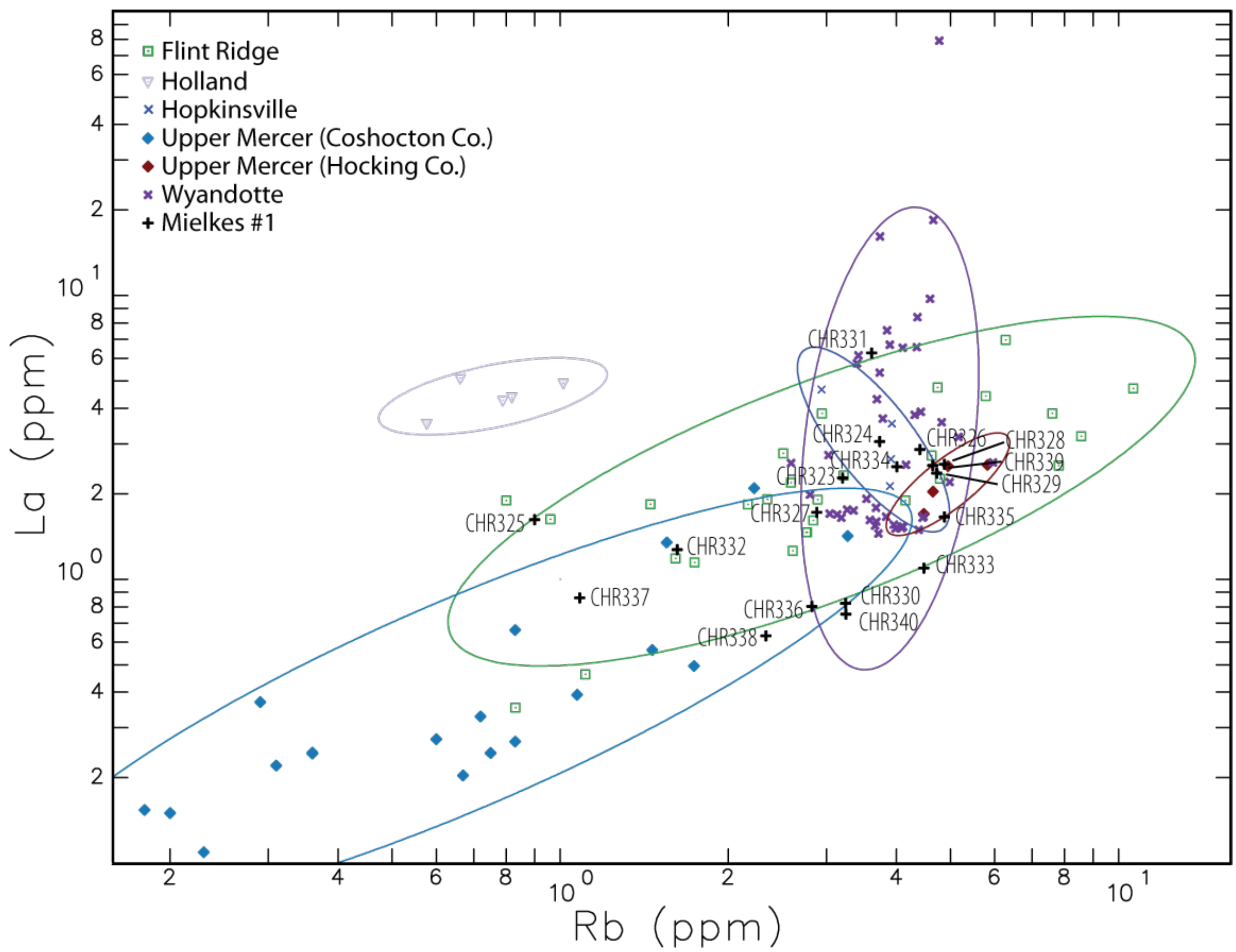

Figure 8. Bivariate plot of La and Rb showing Mielke #1 artifacts visually classified as Wyandotte chert projected against source groups for Flint Ridge, Holland, Hopkinsville, Upper Mercer, and Wyandotte cherts. Ellipses are plotted at the 90% confidence interval.

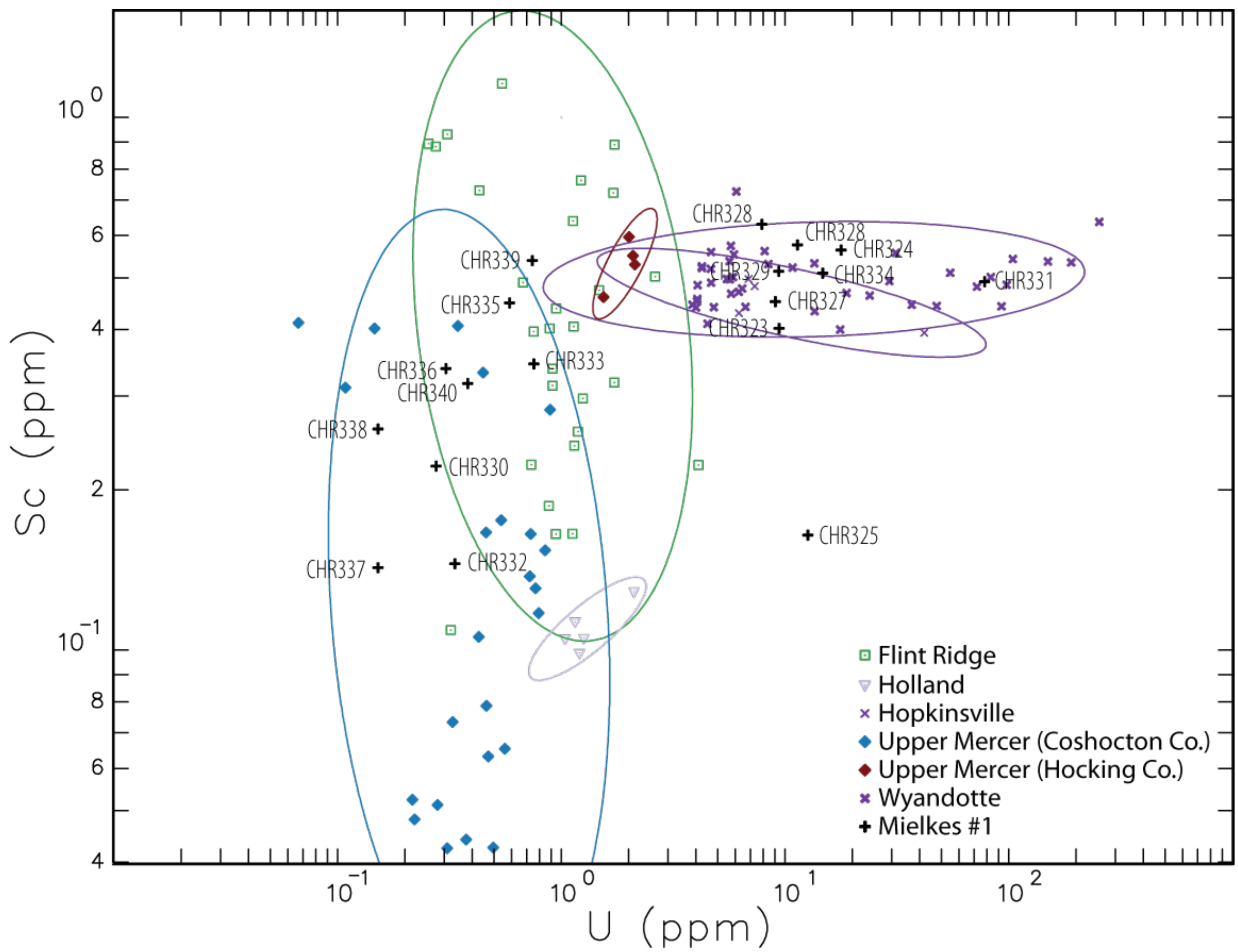

Figure 9. Bivariate plot of Sc and U showing Mielke #1 artifacts visually classified as Wyandotte chert projected against source groups for Flint Ridge, Holland, Hopkinsville, Upper Mercer, and Wyandotte cherts. Ellipses are plotted at the 90% confidence interval.

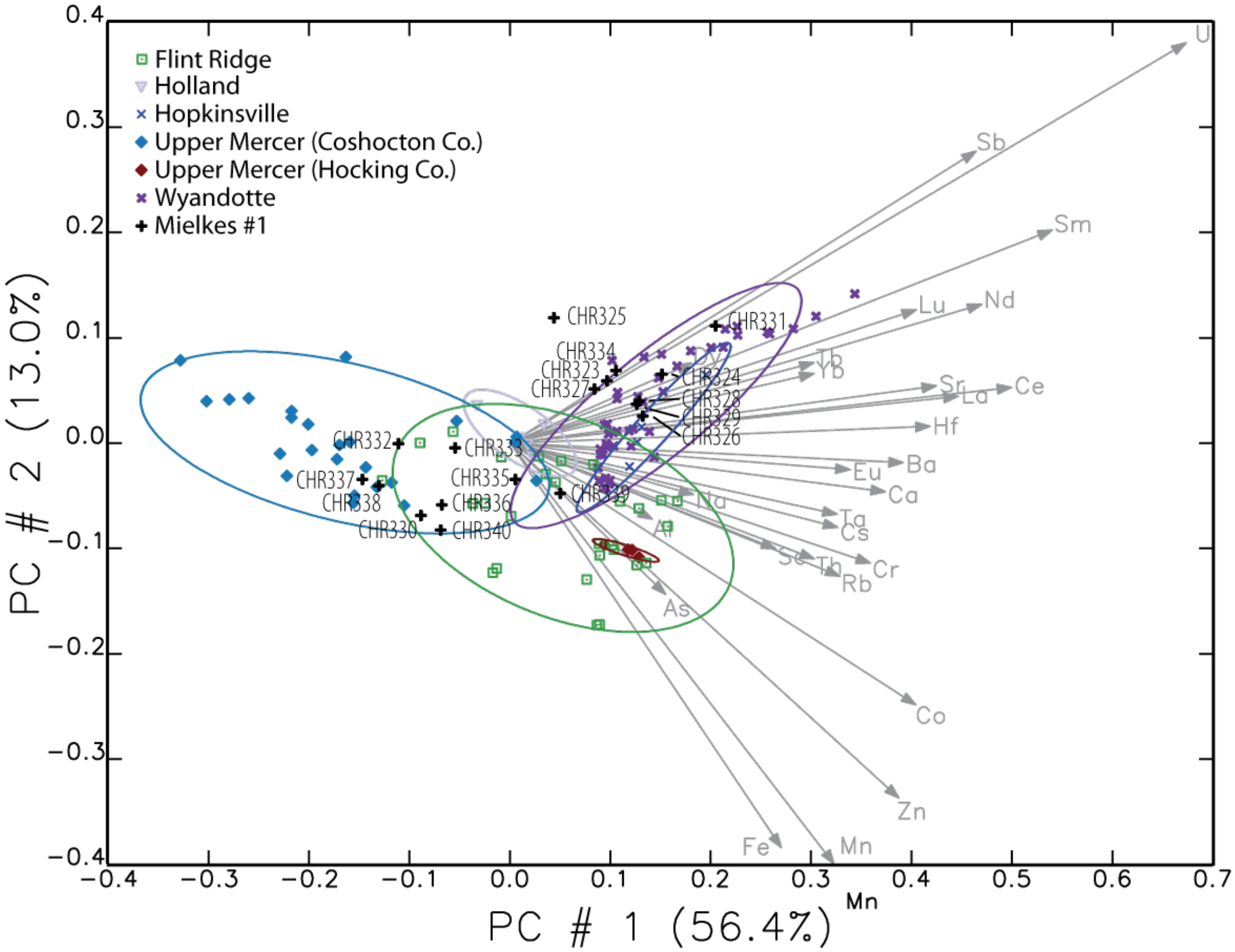

Figure 10. Principal components biplot showing Mielke #1 artifacts visually classified as Wyandotte chert projected against source groups for Flint Ridge, Holland, Hopkinsville, Upper Mercer, and Wyandotte cherts. Ellipses are plotted at the 90% confidence interval.

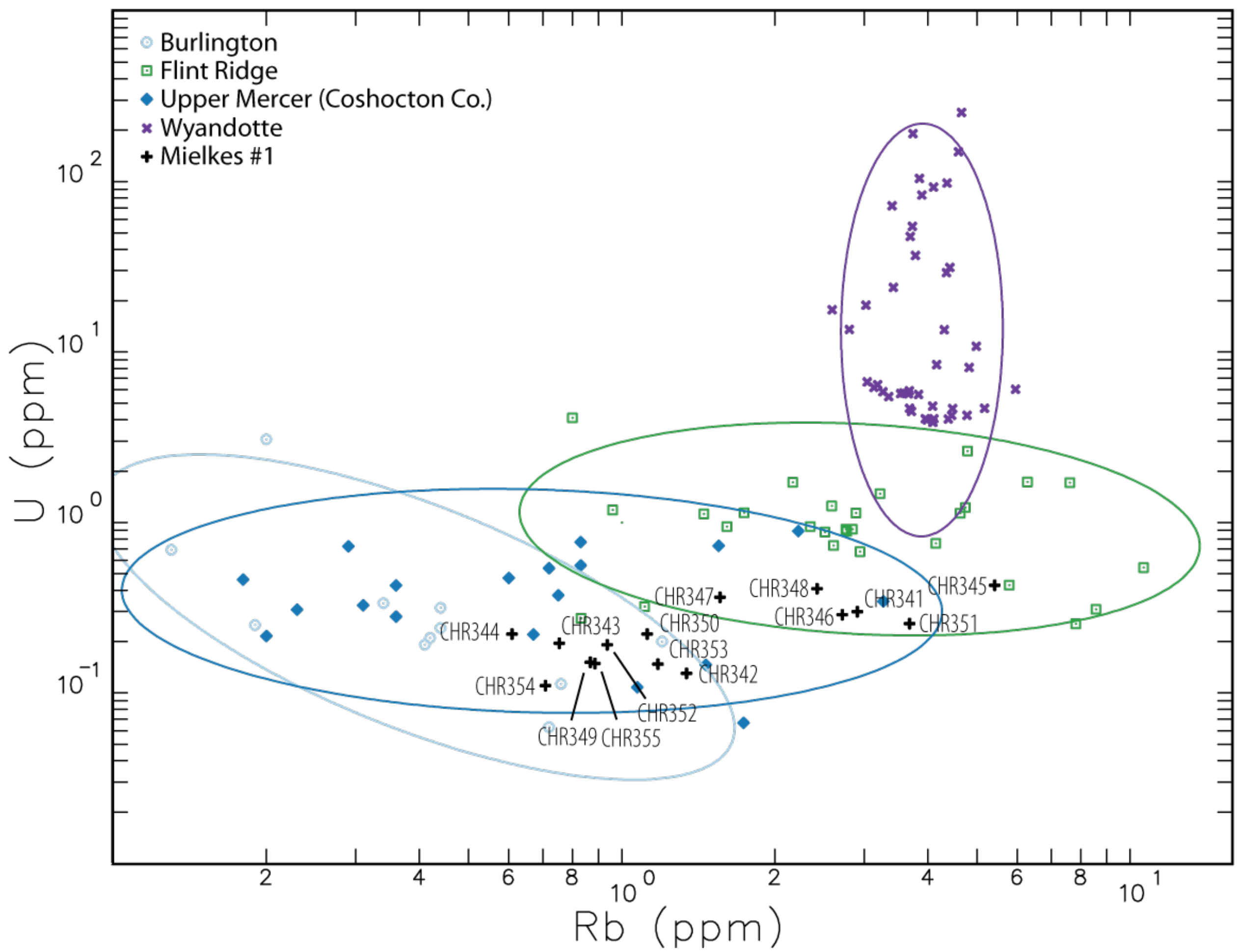

Figure 11. Bivariate plot of U and Rb showing Mielke #1 artifacts visually classified as gray/white chert projected against source groups for Burlington, Flint Ridge, Upper Mercer, and Wyandotte cherts. Ellipses are plotted at the 90% confidence interval.

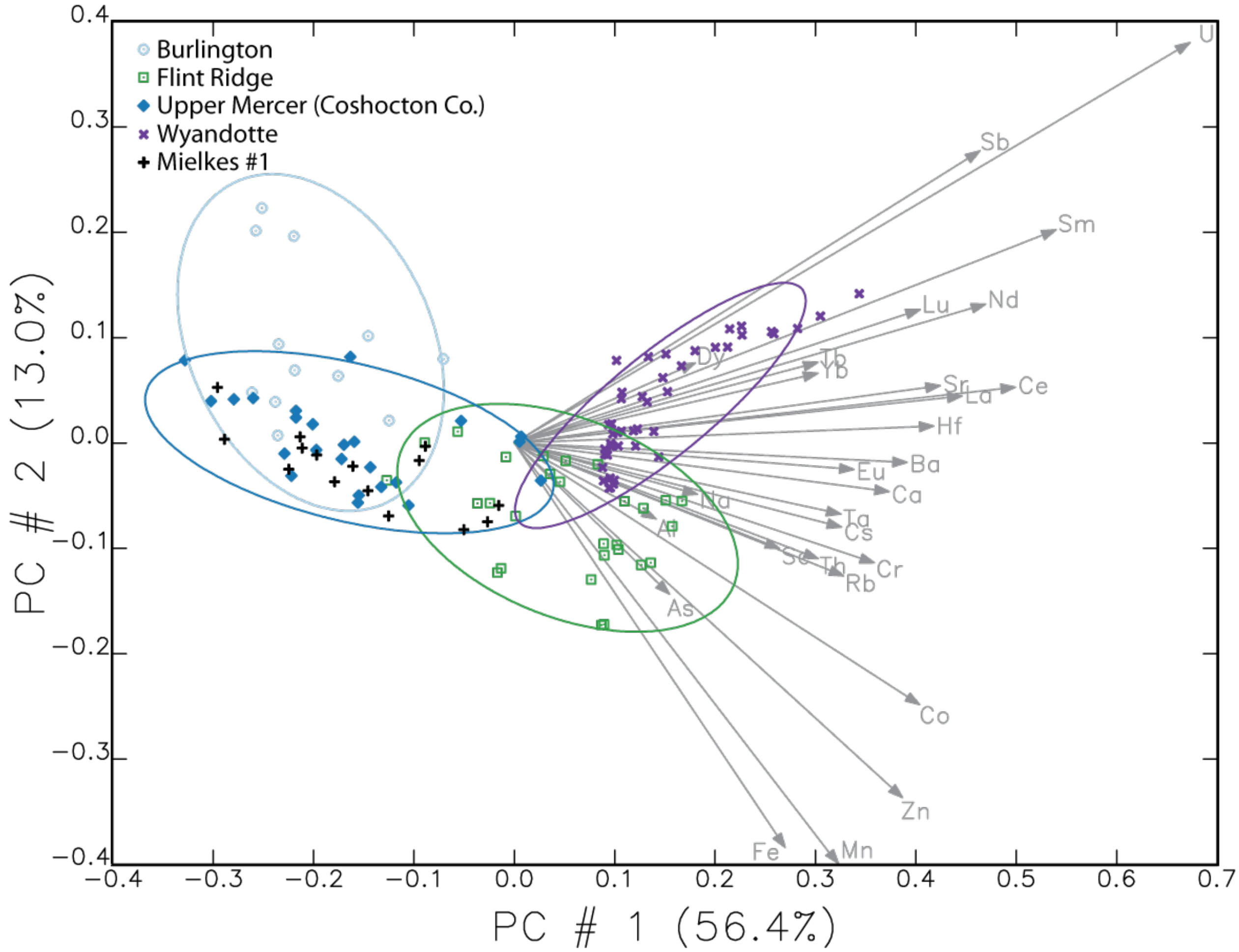

Figure 12. Principal components biplot showing Mielke #1 artifacts visually classified as gray/white chert projected against source groups for Burlington, Flint Ridge, Upper Mercer, and Wyandotte cherts. Ellipses are plotted at the 90% confidence interval.

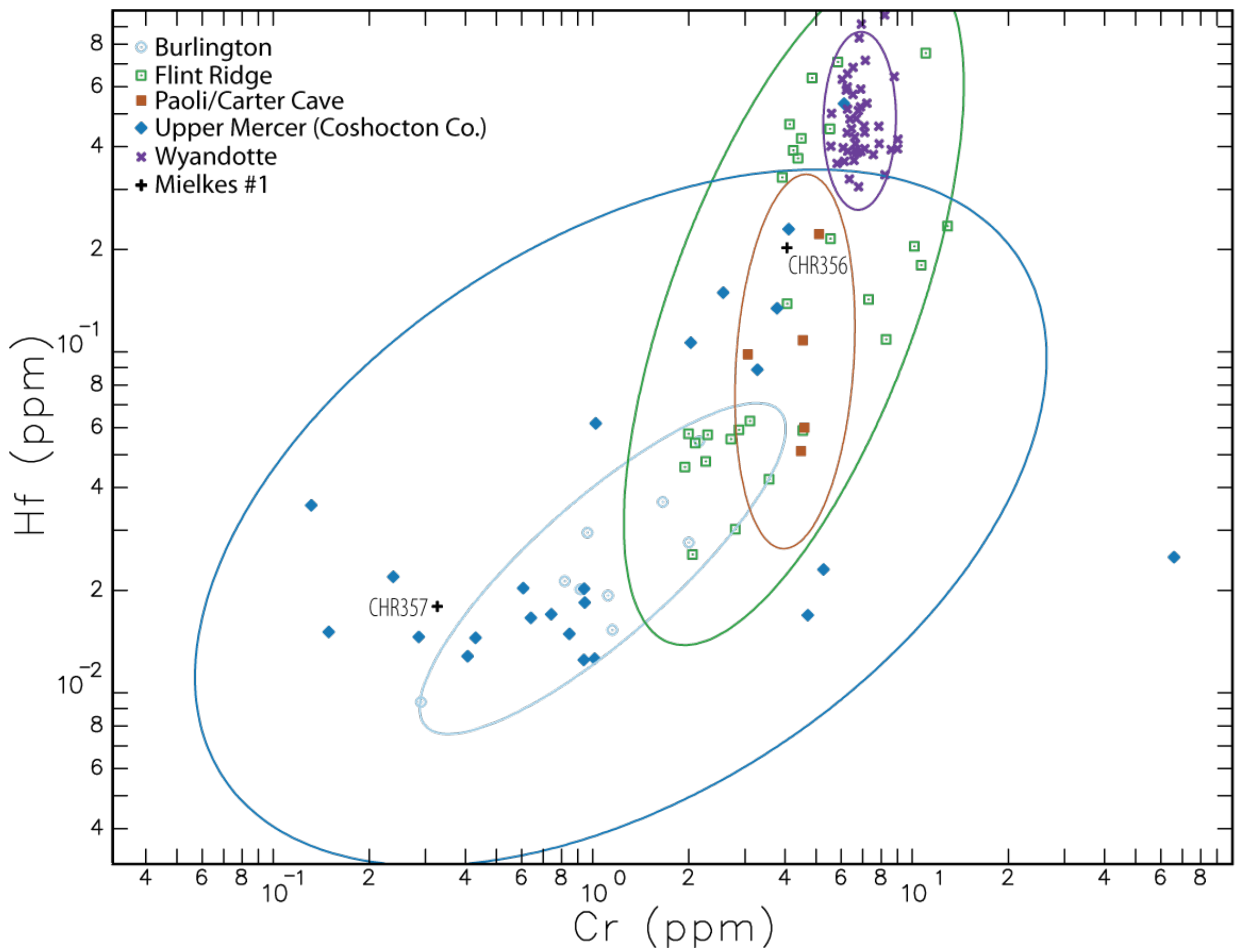

Figure 13. Bivariate plot of Hf and Cr showing Mielke #1 artifacts visually classified as Paoli (Carter Cave) chert projected against source groups for Burlington, Flint Ridge, Upper Mercer, and Wyandotte cherts and previously analyzed artifacts classified as Paoli chert. Ellipses are plotted at the 90% confidence interval.

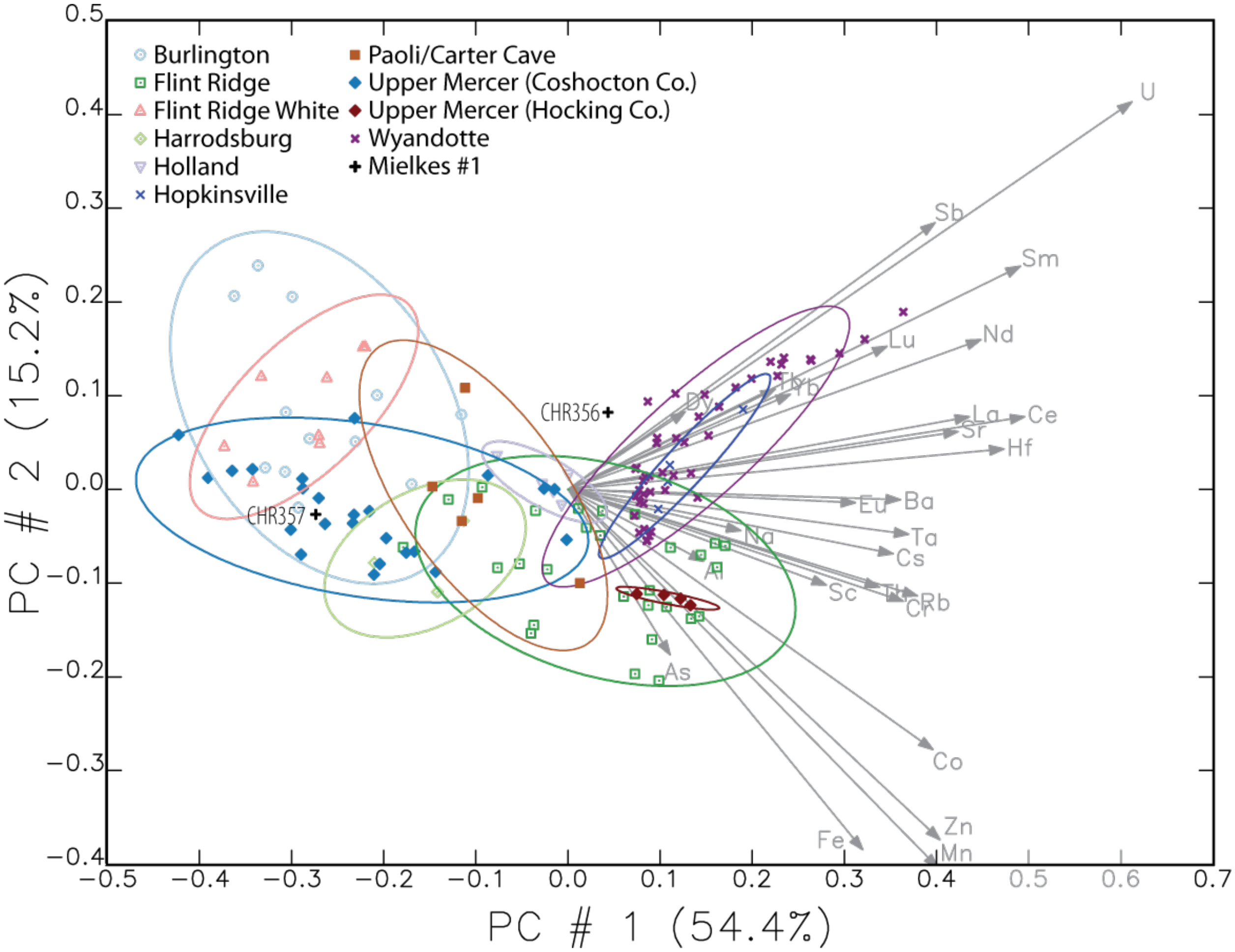

Figure 14. Principal components biplot showing Mielke #1 artifacts visually classified as Paoli (Carter Cave) chert projected against source groups for sources discussed herein, as well as for previously analyzed artifacts classified as Paoli chert. Ellipses are plotted at the 90% confidence interval.

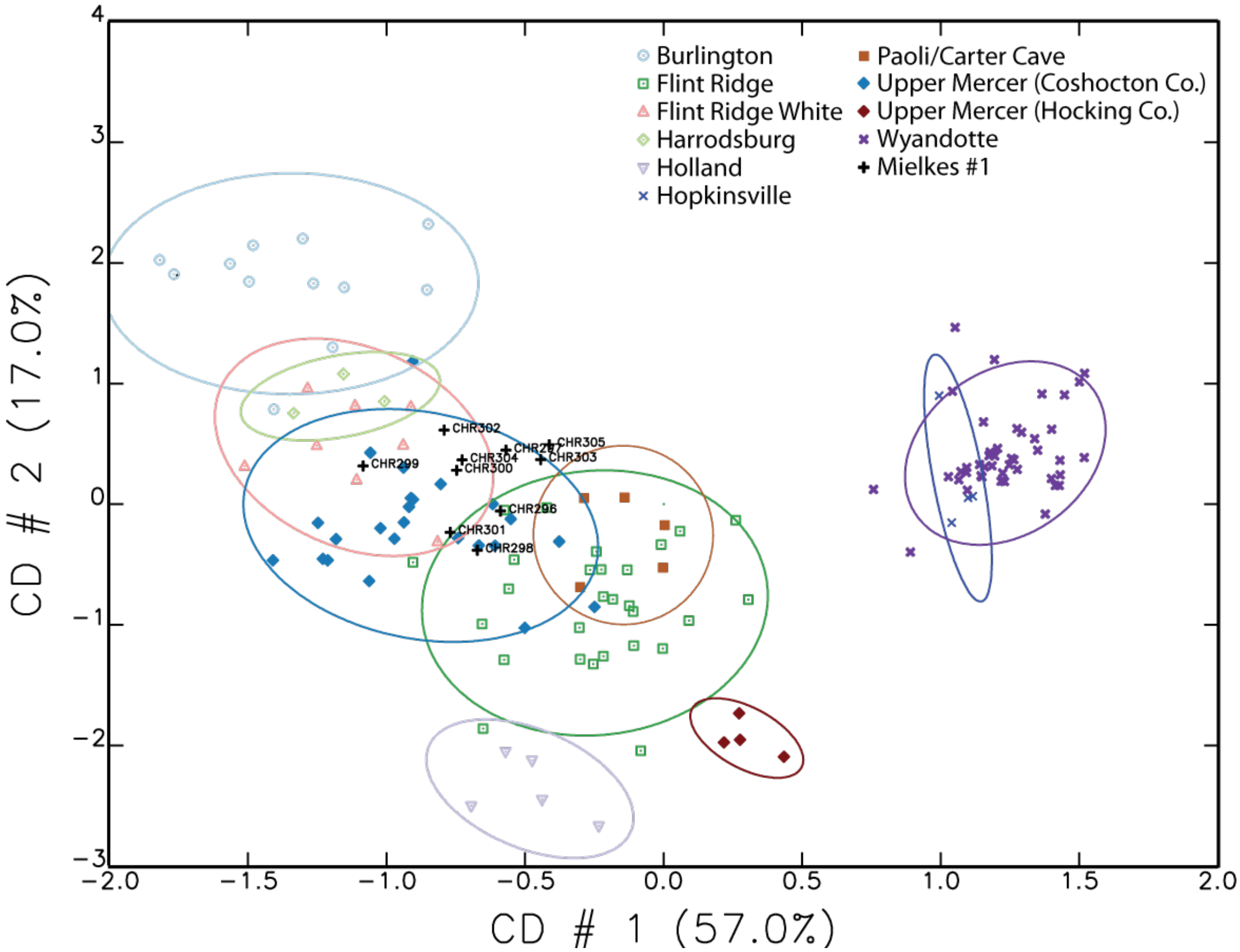

Figure 15. Plot of the first two canonical discriminant functions, describing 74% of the variation between source groups, of the chert sources discussed here as well as the artifacts visually classified as Harrodsburg chert. Ellipses plotted at the 90% confidence interval.

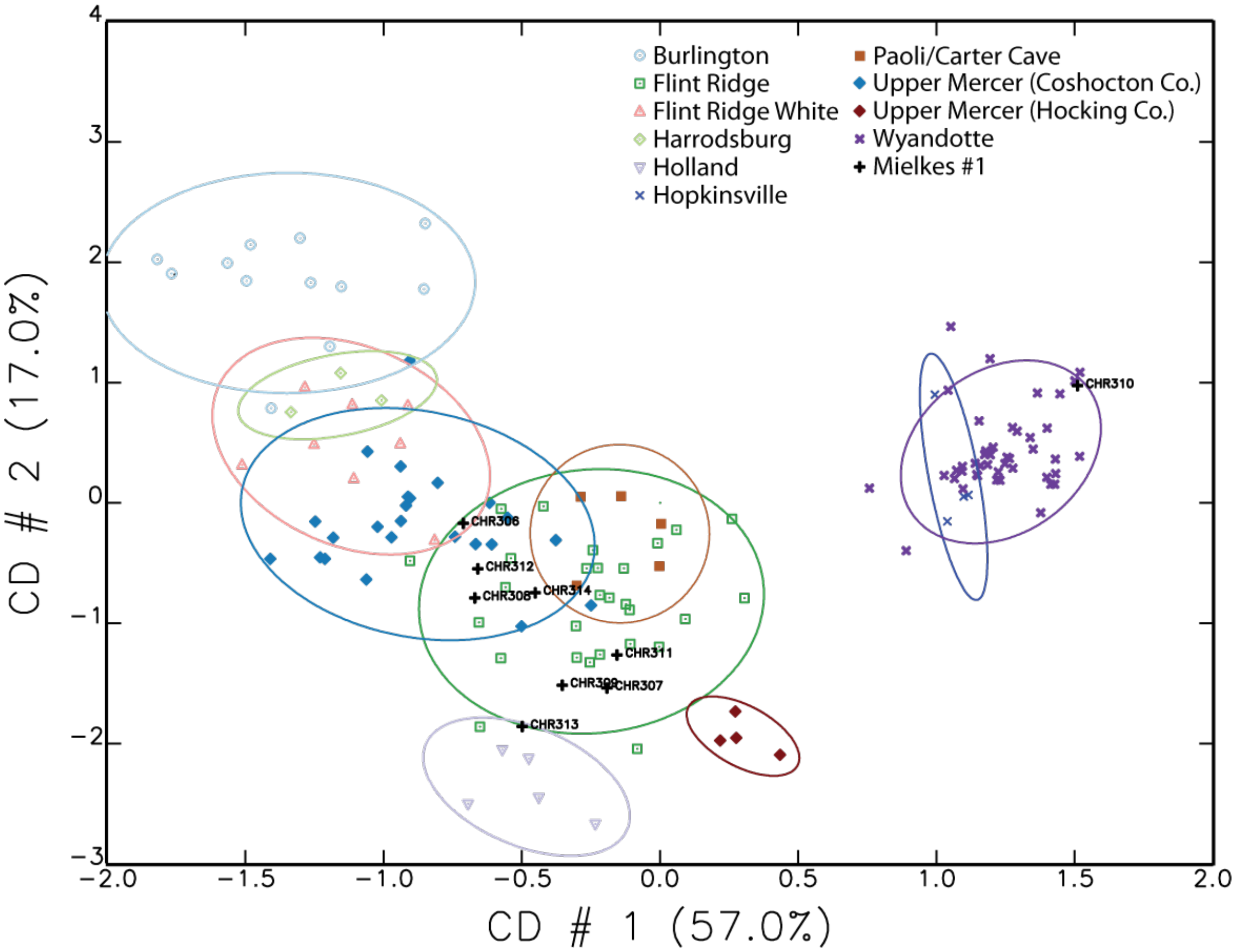

Figure 16. Plot of the first two canonical discriminant functions, describing 74% of the variation between source groups, of the chert sources discussed here as well as the artifacts visually classified as Upper Mercer chert. Ellipses plotted at the 90% confidence interval.

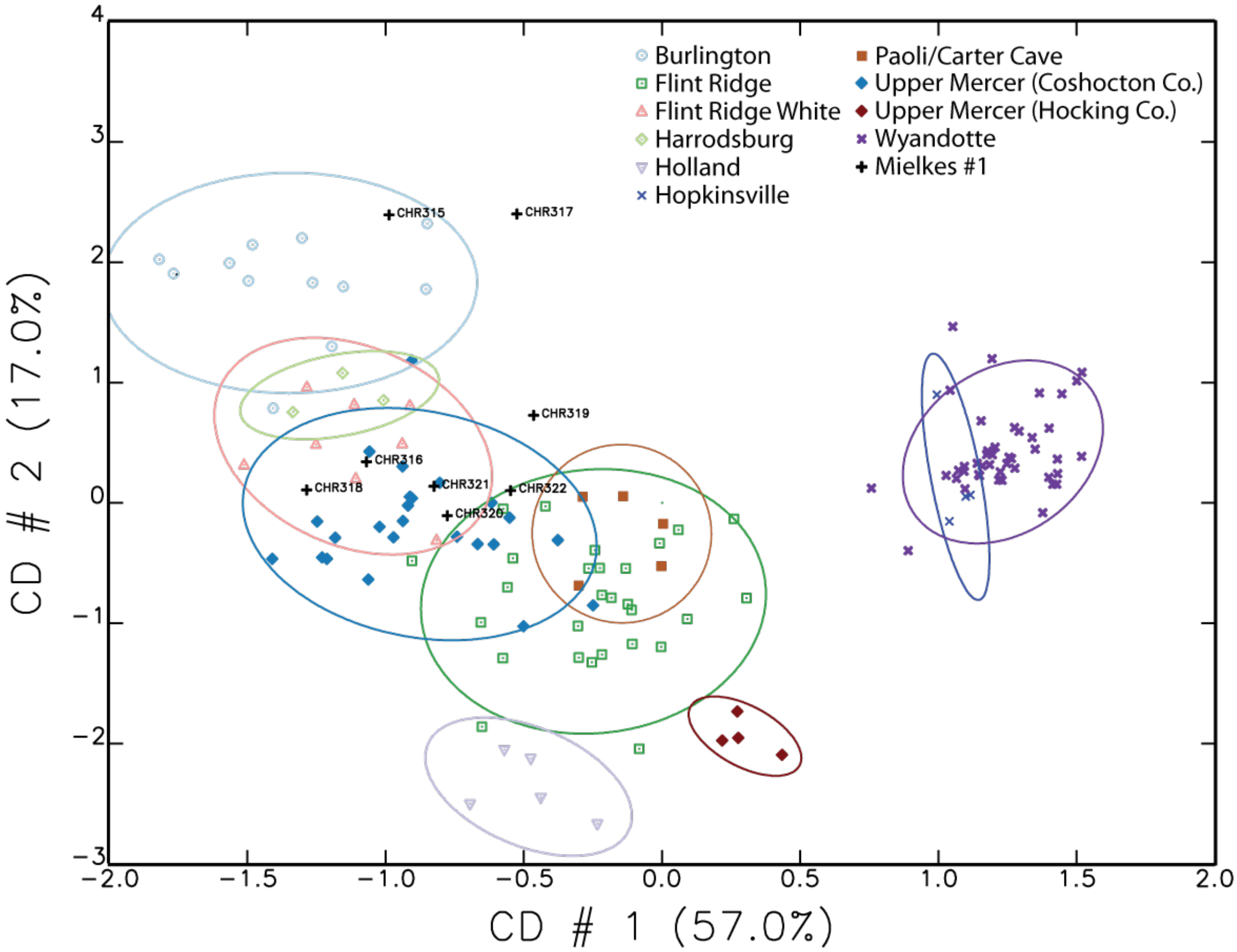

Figure 17. Plot of the first two canonical discriminant functions, describing 74% of the variation between source groups, of the chert sources discussed here as well as the artifacts visually classified as Flint Ridge chert. Ellipses plotted at the 90% confidence interval.

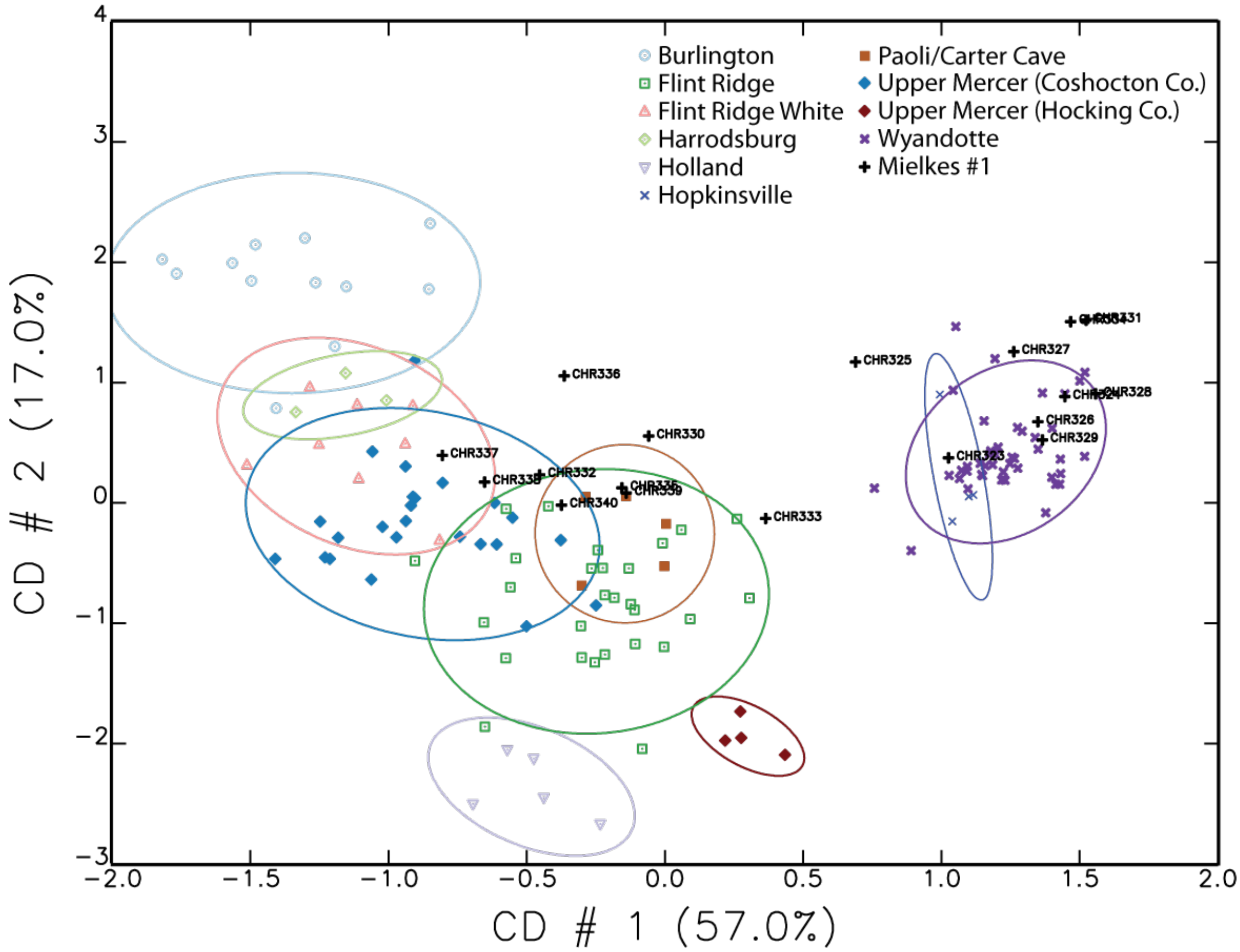

Figure 18. Plot of the first two canonical discriminant functions, describing 74% of the variation between source groups, of the chert sources discussed here as well as the artifacts visually classified as Wyandotte chert. Ellipses plotted at the 90% confidence interval.

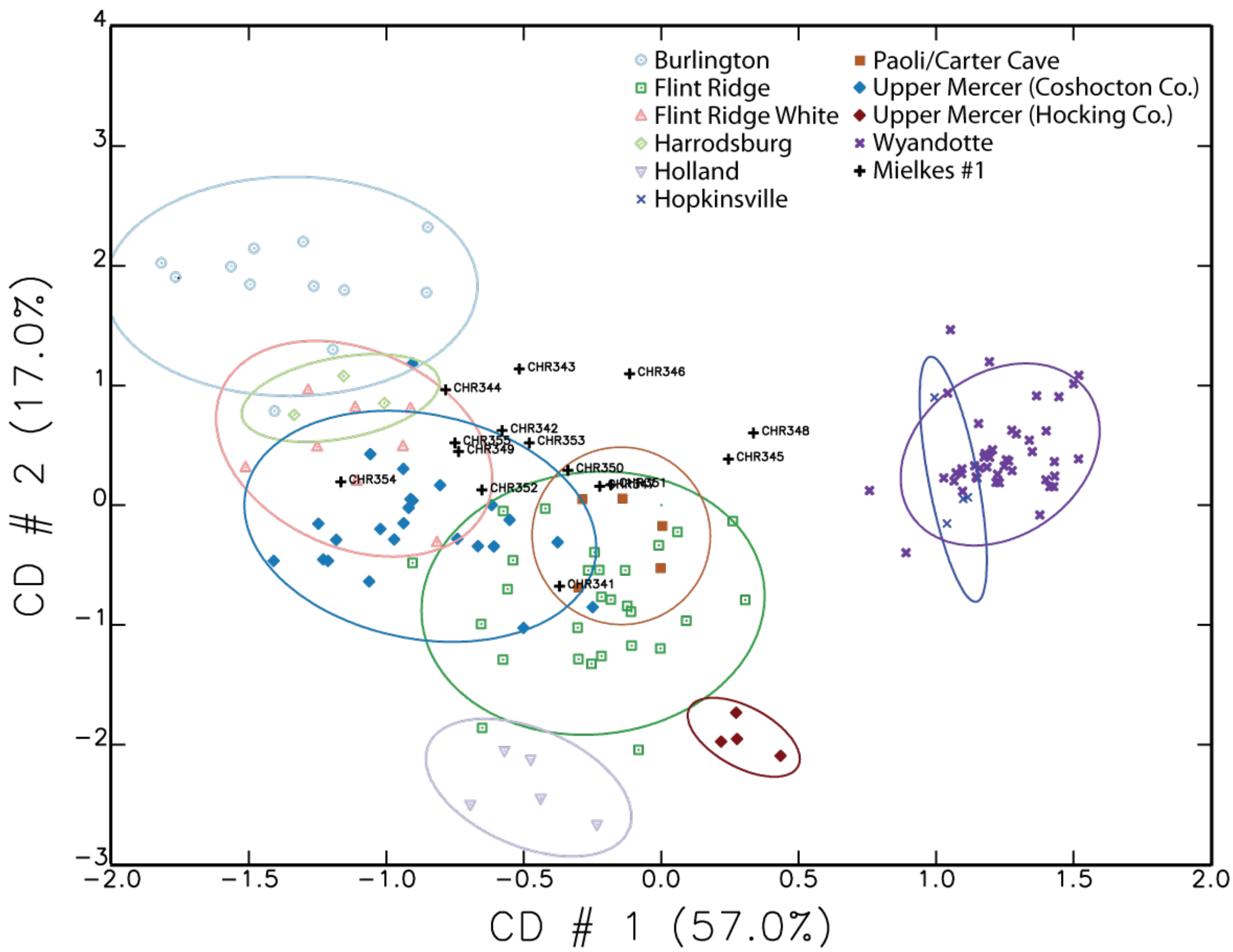

Figure 19. Plot of the first two canonical discriminant functions, describing 74% of the variation between source groups, of the chert sources discussed here as well as the artifacts visually classified as gray-white chert. Ellipses plotted at the 90% confidence interval.

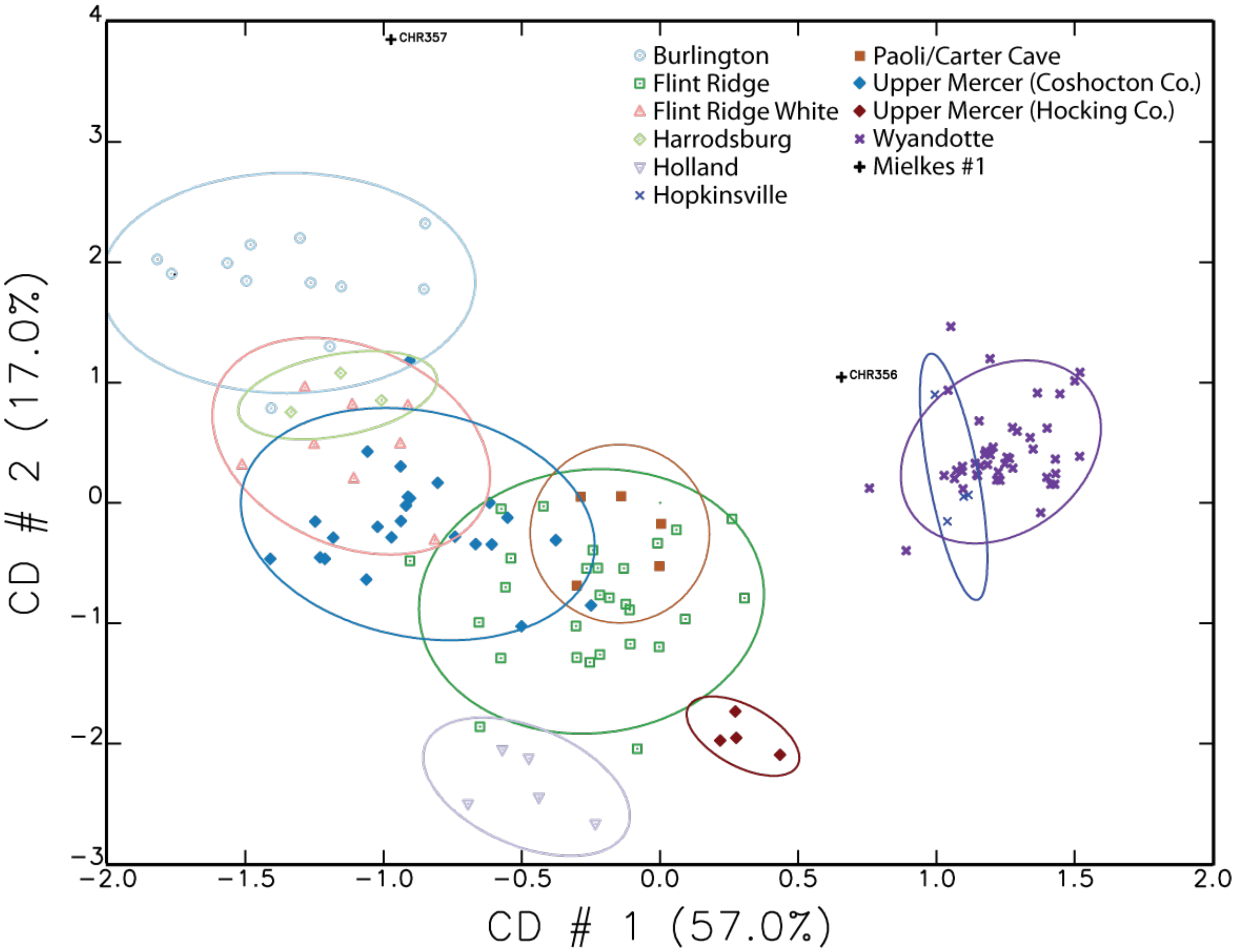

Figure 20. Plot of the first two canonical discriminant functions, describing 74% of the variation between source groups, of the chert sources discussed here as well as the artifacts visually classified as Paoli (Carter Cave) chert. Ellipses plotted at the 90% confidence interval.